NBER WORKING PAPER SERIES

VALUING THE GLOBAL MORTALITY CONSEQUENCES OF CLIMATE CHANGE ACCOUNTING FOR ADAPTATION COSTS AND BENEFITS

Tamma A. Carleton
Amir Jina
Michael T. Delgado
Michael Greenstone
Trevor Houser
Solomon M. Hsiang
Andrew Hultgren
Robert E. Kopp
Kelly E. McCusker
Ishan B. Nath
James Rising
Ashwin Rode
Hee Kwon Seo
Arvid Viaene
Jiacan Yuan
Alice Tianbo Zhang

Working Paper 27599
http://www.nber.org/papers/w27599

NATIONAL BUREAU OF ECONOMIC RESEARCH
1050 Massachusetts Avenue
Cambridge, MA 02138
July 2020

This project is an output of the Climate Impact Lab that gratefully acknowledges funding from the Energy Policy Institute of Chicago (EPIC), International Growth Centre, National Science Foundation, Sloan Foundation, Carnegie Corporation, and Tata Center for Development. Tamma Carleton acknowledges funding from the US Environmental Protection Agency Science To Achieve Results Fellowship (#FP91780401). We thank Trinetta Chong, Greg Dobbels, Diana Gergel, Radhika Goyal, Simon Greenhill, Dylan Hogan, Azhar Hussain, Theodor Kulczycki, Brewster Malevich, Sébastien Annan Phan, Justin Simcock, Emile Tenezakis, Jingyuan Wang, and Jong-kai Yang for invaluable research assistance during all stages of this project, and we thank Megan Landín, Terin Mayer, and Jack Chang for excellent project management. We thank David Anthoff, Max Auffhammer, Olivier Deschênes, Avi Ebenstein, Nolan Miller, Wolfram Schlenker, and numerous workshop participants at University of Chicago, Stanford, Princeton, UC Berkeley, UC San Diego, UC Santa Barbara, University of Pennsylvania, University of San Francisco, University of Virginia, University of Wisconsin-Madison, University of Minnesota Twin Cities, NBER Summer Institute, LSE, PIK, Oslo University, University of British Columbia, Gothenburg University, the European Center for Advanced Research in Economics and Statistics, the National Academies of Sciences, and the Econometric Society for comments, suggestions, and help with data.

Valuing the Global Mortality Consequences of Climate Change Accounting for Adaptation Costs and Benefits

Tamma A. Carleton, Amir Jina, Michael T. Delgado, Michael Greenstone, Trevor Houser, Solomon M. Hsiang, Andrew Hultgren, Robert E. Kopp, Kelly E. McCusker, Ishan B. Nath, James Rising, Ashwin Rode, Hee Kwon Seo, Arvid Viaene, Jiacan Yuan, and Alice Tianbo Zhang

NBER Working Paper No. 27599
July 2020
JEL No. Q54

ABSTRACT

This paper develops the first globally comprehensive and empirically grounded estimates of mortality risk due to future temperature increases caused by climate change. Using 40 countries' subnational data, we estimate age-specific mortality-temperature relationships that enable both extrapolation to countries without data and projection into future years while accounting for adaptation. We uncover a U-shaped relationship where extreme cold and hot temperatures increase mortality rates, especially for the elderly, that is flattened by both higher incomes and adaptation to local climate (e.g., robust heating systems in cold climates and cooling systems in hot climates). Further, we develop a revealed preference approach to recover unobserved adaptation costs. We combine these components with 33 high-resolution climate simulations that together capture scientific uncertainty about the degree of future temperature change. Under a high emissions scenario, we estimate the mean increase in mortality risk is valued at roughly 3.2% of global GDP in 2100, with today's cold locations benefiting and damages being especially large in today's poor and/or hot locations. Finally, we estimate that the release of an additional ton of CO2 today will cause mean [interquartile range] damages of $36.6 [-$7.8, $73.0] under a high emissions scenario and $17.1 [-$24.7, $53.6] under a moderate scenario, using a 2% discount rate that is justified by US Treasury rates over the last two decades. Globally, these empirically grounded estimates substantially exceed the previous literature's estimates that lacked similar empirical grounding, suggesting that revision of the estimated economic damage from climate change is warranted.

Tamma A. Carleton
Bren School of Environmental
Science & Management
University of California, Santa Barbara
Santa Barbara, CA 93106
tcarleton@uchicago.edu

Amir Jina
Harris School of Public Policy
University of Chicago
1155 East 60th Street
Chicago, IL 60637
and NBER
amirjina@uchicago.edu

Michael T. Delgado
Rhodium Group
647 4th St.
Oakland, CA 94607
mdelgado@rhg.com

Michael Greenstone
University of Chicago
Department of Economics
1126 E. 59th Street
Chicago, IL 60637
and NBER
mgreenst@uchicago.edu

Trevor Houser
Rhodium Group
647 4th St.
Oakland, CA 94607
tghouser@rhg.com

Solomon M. Hsiang
Goldman School of Public Policy
University of California, Berkeley
2607 Hearst Avenue
Berkeley, CA 94720-7320
and NBER
shsiang@berkeley.edu

Andrew Hultgren
University of California at Berkeley
hultgren@berkeley.edu

Robert E. Kopp
Department of Earth and Planetary Sciences
Wright Labs, 610 Taylor Road
Rutgers University
Piscataway, NJ 08854-8066
Robert.Kopp@rutgers.edu

Kelly E. McCusker
Rhodium Group
647 4th Street
Oakland, CA 94607
kmccusker@rhg.com

Ishan B. Nath
Department of Economics
University of Chicago
1126 E. 59th St.
Chicago, IL 60637
inath@uchicago.edu

James Rising
Grantham Research Institute
London School of Economics
London, UK
jarising@gmail.com

Ashwin Rode
Department of Economics
University of Chicago
1126 E. 59th St.
Chicago, IL 60637
aarode@uchicago.edu

Hee Kwon Seo
University of Chicago
Booth School of Business
5807 S. Woodlawn Ave.
Chicago, IL 60637
hkseo@chicagobooth.edu

Arvid Viaene
E.CA Economics
Brussels, Belgium
arvid.viaene.db@gmail.com

Jiacan Yuan
Department of Atmospheric
and Oceanic Sciences
Fudan University
Shanghai, China
jiacan.yuan@gmail.com

Alice Tianbo Zhang
Department of Economics
Williams School of Commerce,
Economics, and Politics
Washington and Lee University
Huntley 304
Lexington, VA 24450
atzhang@wlu.edu

An online appendix is available at http://www.nber.org/data-appendix/w27599

1 Introduction

Understanding the likely global economic impacts of climate change is of tremendous practical value to both policymakers and researchers. On the policy side, decisions are currently made with incomplete and inconsistent information on the societal benefits of greenhouse gas emissions reductions. These inconsistencies are reflected in global climate policy, which is at once both lenient and wildly inconsistent. To date, the economics literature has struggled to mitigate this uncertainty, lacking empirically founded estimates of the economic damages from climate change. This problem is made all the more difficult because emissions today influence the global climate for hundreds of years, as Figure 1 illustrates. Thus, any reliable estimate of the damage from climate change must include long-run projections of economic impacts at global scale.

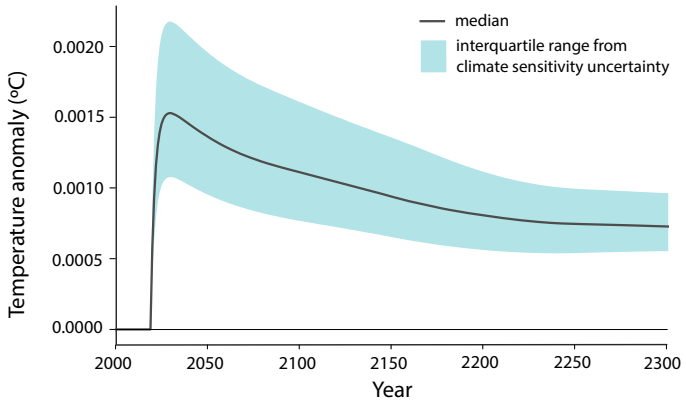

Figure 1: Temperature change due to a marginal emissions pulse in 2020 persists for centuries. The impact of a 1GtC emissions pulse (equivalent to 3.66Gt CO_2) pulse of CO_2 in 2020 on temperature is shown. Median change is the difference in temperature of the "pulse" scenario relative to a high-emissions baseline scenario. The levels are anomalies in global mean surface temperature (GMST) in Celsius using our modification of the FAIR climate model. The shaded area indicates the inter-quartile range due to uncertainty in the climate's sensitivity to CO_2 (see Section 6 for details).

Decades of study have accumulated numerous insights and important findings regarding the economics of climate change, both theoretically and empirically, but a fundamental gulf persists between the two main types of analyses pursued. On the one hand, there are stylized models able to capture the global and multi-century nature of problem, such as "integrated assessment models" (IAMs) (e.g., Nordhaus, 1992; Tol, 1997; Stern, 2006), whose great appeal is that they provide an answer to the question of what the global costs of climate change will be. However, the many necessary assumptions of IAMs weaken the authority of these answers. On the other hand, there has been an explosion of highly resolved empirical analyses whose credibility lie in their use of real world data and careful econometric measurement (e.g., Schlenker and Roberts, 2009; Deschênes and Greenstone, 2007).[1] Yet these analyses tend to be limited in scope and rely on short-run changes in weather that might not fully account for adaptation to gradual climate change (Hsiang, 2016). At its core, this dichotomy persists because researchers have traded off between being complete in scale and scope or investing heavily in data collection and analysis. The result is that no study has delivered estimated effects of climate

[1]For a comprehensive review, see Dell, Jones, and Olken (2014); Carleton and Hsiang (2016); Auffhammer (2018b).

change that are at the scale of IAMs, while simultaneously being grounded in detailed econometric analyses using high-resolution globally representative micro-data.

The paper sets out to accomplish two major goals that require resolving the tension between these approaches in the context of mortality risk due to climate change. Specifically, it strives to provide the temporal and global scale of IAMs, but transparently built upon highly resolved econometric foundations. In so doing, it aims to account for both the benefits and costs of adaptation. The first goal is to produce local and global estimates of the mortality risk of climate change and its monetized value. The spatial resolution, based on dividing the world into 24,378 regions,[2] marks a substantial improvement upon existing IAMs, which represent (at most) 16 heterogeneous global regions (Tol, 1997). Using these calculations, we are able to accomplish the second goal, which is to estimate marginal willingness-to-pay (MWTP) to avoid the alteration of mortality risk associated with the release of an additional metric ton of CO_2. We call this the excess mortality "partial" social cost of carbon (SCC); a "full" SCC would encompass impacts across all affected outcomes.

In order to make these contributions, the analysis overcomes four fundamental challenges that have prevented the construction of empirically-derived and complete estimates of the costs of climate change to date. The first two of these challenges are due to the global extent and long timescale of both the causes and the impacts of climate change. For the first challenge, we note that CO_2 is a global pollutant, meaning that the costs of climate change must necessarily be considered at a global scale; anything less will lead to an incomplete estimate of the costs. The second challenge is that populations exhibit various levels of adaptation to current climate across space and adaptation levels are likely to be different in the future as populations become exposed to changes in their local climate. The extent to which investments in adaptation can limit the impacts of climate change is a critical component of cost estimates; ignoring this would lead to overstating costs.

We address both of these challenges simultaneously with a combination of extensive data and an econometric approach that models heterogeneity in the mortality-temperature relationship. We estimate this relationship using the most comprehensive dataset ever collected on annual, sub-national mortality statistics from 41 countries that cover 55% of the global population. These data allow us to estimate age-specific mortality-temperature relationships with substantially greater resolution and coverage of the human population than previous studies; the most comprehensive econometric analyses to date have been for a few countries within a single region or individual cities from several countries. The analysis relies on inter-annual variation in temperature and uncovers a plausibly causal U-shaped relationship where extreme cold and hot temperatures increase mortality rates, especially for the elderly (those aged 65 and older).

We quantify the benefits of adaptation to gradual climate change and the benefits of projected future income growth by jointly modeling heterogeneity in the mortality-temperature response function with respect to the long-run climate (e.g., Auffhammer, 2018a) and income per capita (e.g., Fetzer, 2014). This cross-sectional modeling of heterogeneity allows us to predict the structure of the mortality-temperature relationship across locations where we lack data, as well as into the future, both of which are necessary to assess the global impacts of climate change. Such out-of-sample extrapolation of temperature-mortality relationships delivers the first empirically-based approach to including

[2]In the U.S., these impact regions map onto a county.

these populations in global climate impacts analysis, although a causal interpretation requires stronger econometric assumptions. Using readily available data and projections for current and future climate, income, and population projections, we estimate that the effect of an additional very hot day (35°C / 95°F) on elderly mortality is ∼50% larger in regions of the world where mortality data are unavailable. This finding underlines that current estimates may understate climate change impacts because they disproportionately rely on data from wealthy economies and temperate climates. Furthermore, accounting for changing mortality-temperature relationships is crucial to projecting the effect of warming in the future, as we expect the mortality consequences of heat to decline over time due to adaptations that individuals are predicted to undertake in response to warmer climates and higher incomes. Consistent with this intuition we find that climate adaptation and income growth have substantial benefits, marking a departure from previous literature that has often assumed that the mortality-temperature relationship was constant over space and time (e.g., Deschênes and Greenstone, 2011).

The third challenge is that the adaptation responses discussed in the previous paragraph are costly, and these costs, along with the direct mortality impacts, must be accounted for in a full assessment of climate change impacts. We develop a general revealed preference method to estimate the costs incurred to achieve the benefits from adapting to climate change, even though these costs cannot be directly observed. This is a critical step because a full accounting of the mortality-related costs of climate change necessarily accounts for the direct mortality impacts, the benefits of adaptation, and the opportunity costs of all resources deployed in order to achieve those adaptations. This is an advance on the previous literature that has either quantified adaptation benefits without estimating costs (e.g., Heutel, Miller, and Molitor, 2017) or tried to measure the costs of individual adaptations (e.g., Barreca et al., 2016). The latter approach is informative of individual costs, but poorly equipped to measure total adaptation costs, because the range of potential responses to warming – whether defensive investments (e.g., building cooling centers) or compensatory behaviors (e.g. exercising earlier in the morning) – is enormous, making a complete enumeration of their costs extraordinarily challenging.

The revealed preference approach is based on the assumption that individuals undertake adaptation investments when the expected benefits exceed the costs and that for the marginal investment, benefits and costs are equal. Because we can empirically observe adaptation benefits by measuring reduced mortality sensitivities to temperature, we can therefore infer their marginal cost. Then by integrating marginal costs, we can compute total costs for non-marginal climate changes. A simplified but illustrative example comes from comparing Seattle, WA and Houston, TX, which have similar income levels, but very different climates: on average, Seattle has less than 1 day per year where the daily average temperature exceeds 30°C (85°F), while Houston experiences over 8 of these days annually.[3] Our empirical analysis below finds that Houston is relatively adapted to this hotter climate, with an individual hot day leading to much lower mortality than in temperate Seattle. By revealed preference, it must be the case that the costs required to achieve Houston-like adaptation exceeds the value of the lives Seattle would save by adopting similar practices. Similarly, the costs of adapting in Houston must be less than or equal to the value of the additional deaths that they would otherwise have to endure. These bounds shrink for smaller differences in climate (e.g. Seattle vs. Tacoma), such that we can show that for infinitesimally small differences in climate, these bounds collapse to

[3]These values of *average* daily temperature are calculated from the GMFD dataset, described in Section 3.

a single value where the estimable marginal benefits and unobserved marginal costs are equal. Using this result, we are able to reconstruct non-marginal adaptation costs for each location, relying only on empirically recovered reduced-form estimates.

Together, addressing these three challenges allows us to achieve the first goal of this analysis: to develop measures of the full mortality-related costs of future climate change for the entire world, reflecting both the direct mortality costs accounting for adaptation and all adaptation costs. This exercise is done using 33 global climate models that together reflect current scientific uncertainty about the degree of temperature change[4] and results are expressed in "death equivalents", i.e., the number of deaths plus the adaptation costs incurred expressed in avoided deaths. We find that under a high emissions scenario (i.e., Representative Concentration Pathway (RCP) 8.5, in which CO_2 emissions growth is sustained) and a socioeconomic scenario with future global income and population growth rates approximately matching recent observations (i.e., Shared Socioeconomic Pathway (SSP) 3), the mean estimate of the total mortality burden of climate change is projected to be worth 85 death equivalents per 100,000, at the end of the century. Accounting for econometric and climate uncertainty leads to an interquartile range of [16, 121].[5] This is equal to roughly 3.2% of global GDP at the end of the century when death equivalents are valued using an age-varying value of a statistical life (VSL). Further, failing to account for income and climate adaptation would overstate the mortality costs of climate change by a factor of about 2.6, on average.

The analysis uncovers substantial heterogeneity in the full mortality costs of climate change around the globe. For example, mortality risk in Accra, Ghana is projected to increase by 19% of its current annual mortality rate at the end of the century under a high emissions scenario, while Oslo, Norway is projected to experience a decrease in mortality risk due to milder winters that is equal to 28% of its current annual mortality rate today (United Nations, 2017). Further, the share of the full mortality-related costs of climate change that are due to deaths, rather than adaptation costs, is 86% globally but varies greatly, with poor countries disproportionately experiencing impacts through deaths and wealthy countries disproportionately experiencing impacts through adaptation costs.

The last of the four challenges facing the literature is the calculation of an SCC that is based upon empirical evidence, the calculation of which is the second goal of our analysis. We develop and implement a framework to estimate the excess mortality partial SCC using empirically-based projections. The mortality partial SCC is defined as the marginal willingness-to-pay to avoid an additional ton of CO_2. A central element of this procedure is the construction of empirically grounded "damage functions," (Hsiang et al., 2017), each of which describes the costs of excess mortality risk in a given year as a function of the overall level of global climate change. Such damage functions have played a central role in the analysis of climate change as an economic problem since seminal work by Nordhaus (1992), but existing estimates have been criticized for having little or no empirical foundation (Pindyck, 2013). To our knowledge, ours is the first globally representative and empirically grounded partial damage function, enabling us to calculate a partial SCC when combined with a climate model.

Our estimates imply that the excess mortality partial SCC is roughly $36.6 (in 2019 USD) with

[4] See Burke et al. (2015) for a discussion of combining physical climate uncertainty with econometric estimates.

[5] For reference, all cancers are responsible for approximately 125 deaths per 100,000 globally today (WHO, 2018). Of course, the full costs of cancer, including all adaptations incurred to avoid risk, would be even larger if expressed in death equivalents.

a high emissions scenario (RCP8.5) under a 2% discount rate and using an age-varying VSL. This value falls to $17.1 with a moderate emissions scenario (i.e., Representative Concentration Pathway (RCP) 4.5, in which CO_2 emissions are stable through 2050 and then decline), due to the nonlinearity of estimated damage functions. The respective interquartile ranges are [-$7.8, $73.0] for RCP8.5 and [-$24.7, $53.6] for RCP4.5. These assumptions regarding discount rate and VSL are justified by US Treasury rates over the last two decades[6] and by standard economic reasoning regarding mortality risk valuation (Jones and Klenow, 2016; Murphy and Topel, 2006), respectively. However, under a higher discount rate of 3% and an age-invariant VSL, valuation assumptions used by the United States Government to set the SCC in 2009, the mortality partial SCC is approximately $22.1 [-$5.6, $53.4] under RCP8.5 and $6.7 [-$15.7, $32.1] under RCP4.5.

These empirically grounded estimates of the costs of climate-induced mortality risks substantially exceed available estimates from leading IAMs. For example, the total mortality-related damages from climate change under RCP8.5 in 2100 amount to about 49-135% of the comparable damages reported for *all sectors of the economy* in the IAMs currently determining the U.S. SCC (Interagency Working Group on Social Cost of Carbon, 2010). When considering the full discounted stream of damages from the release of an additional metric ton of CO_2, this paper's excess mortality partial SCC with a high emissions scenario amounts to ∼73% of the Obama Administration's *full* SCC (under a 2% discount rate and age-varying VSL); this value falls to ∼44% when using a 3% discount rate and age-invariant VSL.

The rest of this paper is organized as follows: Section 2 outlines a conceptual framework for the two key problems of the paper: projecting climate damages into the future, accounting for adaptation and its cost, and estimating a mortality partial SCC; Section 3 describes the data used in the estimation of impacts and in the climate change projected impacts; Section 4 details the econometric approach and explains how we extrapolate mortality impacts across space and project them over time while computing adaptation costs and benefits; Section 5 describes the results of the econometric analysis and presents global results from projections that use high-resolution global climate models; Section 6 details the calculation of a damage function based on these projections and computes a mortality partial SCC; Section 7 discusses limitations of the analysis; and Section 8 concludes.

2 Conceptual framework

Climate change is projected to have a wide variety of impacts on well-being, including altering the risk of mortality due to extreme temperatures. The ultimate effect on particular outcomes like mortality rates will be determined by the adaptations that are undertaken. Specifically, as the climate changes, individuals and societies will weigh the costs and benefits of undertaking actions that allow them to exploit new opportunities (e.g., converting land to new uses) and protect themselves against new risks (e.g., investments in air conditioning to mitigate mortality risks). The full cost of climate change, and hence the social cost of carbon, will thus reflect both the realized *direct impacts* (e.g., changes in mortality rates), which depend on the benefits of these adaptations, and *the costs of these adaptations in terms of foregone consumption*. However, to date it has proven challenging to develop a theoretically

[6]The average 10-year Treasury Inflation-Indexed Security value over the available record of this index (2003-present) is 1.01% (Board of Governors of the US Federal Reserve System, 2020).

founded and empirically credible approach to explicitly recover the full costs of climate change and to incorporate such costs into an SCC.[7]

This section develops a simple framework to define (i) the full value of mortality risk due to climate change, and (ii) the mortality partial SCC, such that each reflects both the costs and benefits of adaptation. In both cases, we are able to derive expressions for these objects that are composed of terms that can be estimated with data.

2.1 Setup

We define the *climate* as the joint probability distribution over a vector of possible conditions that can be expected to occur over a specific interval of time. Following the notation of Hsiang (2016), let $\boldsymbol{C}_t$ be a vector of parameters describing the entire joint probability distribution over all relevant climatic variables in time period t (e.g., $\boldsymbol{C}$ might contain the mean and variance of daily average temperature and rainfall, among other parameters). The climate is determined both by natural variations in the climate system, and by the history of anthropogenic emissions. Thus, we write $\boldsymbol{C}_t = \varphi(E_0, E_1, E_2, ...E_t)$ where E_t represents total global greenhouse gas emissions in period t and $\varphi(\cdot)$ is a general function determined by the climate system that links past emissions to present climate.[8]

Define weather realizations as a random vector $\boldsymbol{c}_t$ drawn from a distribution characterized by $\boldsymbol{C}_t$. Emissions therefore influence realized weather by shifting the probability distribution, $\boldsymbol{C}_t$. Mortality risk is a function of both weather $\boldsymbol{c}$ and a composite good $\boldsymbol{b} = \xi(b_1, ..., b_K)$ comprising all b_k, where each b_k is an endogenous economic variable that influences adaptation. The composite $\boldsymbol{b}$ thus captures all adaptive behaviors and investments that interact with individuals' exposure to a warming climate, such as installation of air conditioning and time allocated to indoor activities. Mortality risk is captured by the probability of death during a unit interval of time $f_t = f(\boldsymbol{b}_t, \boldsymbol{c}_t)$.

Consider a single representative global agent who derives utility in all time periods t from consumption of the numeraire good x_t and who faces mortality risk $f_t = f(\boldsymbol{b}_t, \boldsymbol{c}_t)$.[9] Because weather realizations $\boldsymbol{c}_t$ are a random vector, this agent simultaneously chooses consumption of the numeraire x_t and of the composite good $\boldsymbol{b}_t$ in each period to maximize utility given her *expectations* of the weather, subject to an exogenous budget constraint, conditional on the climate.[10] We let $\tilde{f}(\boldsymbol{b}_t, \boldsymbol{C}_t) = \mathbb{E}_{\boldsymbol{c}_t}[f(\boldsymbol{b}_t, \boldsymbol{c}(\boldsymbol{C}_t)) \mid \boldsymbol{C}_t]$ represent the expected probability of death, where $\boldsymbol{c}(\boldsymbol{C})$ is a random vector $\boldsymbol{c}$ drawn from a distribution characterized by $\boldsymbol{C}$. This agent chooses their adaptations by solving:

$$\max_{\boldsymbol{b}_t, x_t} \; u(x_t)\left[1 - \tilde{f}(\boldsymbol{b}_t, \boldsymbol{C}_t)\right] \quad s.t. \;\; Y_t \geq x_t + A(\boldsymbol{b}_t), \tag{1}$$

where climate is determined by the history of emissions, where $A(\boldsymbol{b}_t)$ represents expenditures for all

[7] See Deschênes and Greenstone (2011); Hsiang and Narita (2012); Schlenker, Roberts, and Lobell (2013); Lobell et al. (2014); Guo and Costello (2013); Deschênes, Greenstone, and Shapiro (2017); Deryugina and Hsiang (2017) for different theoretical discussions of this issue and some of the empirical challenges.

[8] For more discussion, see Hsiang and Kopp (2018).

[9] Note that our empirical analysis relies on heterogeneous agents exposed to different climates, realizing different incomes, and exhibiting different demographics. However, for expositional simplicity here we derive the full mortality risk of climate change and the mortality partial SCC using a globally representative agent.

[10] The assumption of exogenous emissions implies that we rule out the possibility that the agent will choose an optimal E^*. This is unrealistic with a single agent. But in practice, the world is comprises a continuum of agents or countries and the absence of coordinated global climate policy today is consistent with agents failing to choose optimal $\boldsymbol{b}^*$.

adaptive investments, and Y is an income we take to be exogenous.[11]

The following framework relies on a key set of assumptions. First, we assume that adaptation costs are a function of technology and do not depend on the climate. Additionally, we assume that $\tilde{f}(\cdot)$ is continuous and differentiable, that markets clear for all technologies and investments represented by the composite good $\boldsymbol{b}$, as well as for the numeraire good x, and that all choices $\boldsymbol{b}$ and x can be treated as continuous. Importantly, Equation 1 is static, because we assume that there is a competitive and frictionless rental market for all capital goods (e.g., air conditioners), so that fixed costs of capital can be ignored, and that all rental decisions are contained in $\boldsymbol{b}$. As long as agents have accurate expectations over their current climate, markets will clear efficiently in each period. Under these assumptions, the first order conditions of Equation 1 define optimal adaptation as a function of income and the climate: $\boldsymbol{b}^*(Y_t, \boldsymbol{C}_t)$, which we sometimes denote below as $\boldsymbol{b}_t^*$ for simplicity.

2.2 The full value of mortality risk due to climate change

We first use the representative agent's problem in Equation 1 to derive an empirically tractable expression for the full value of mortality risk due to climate change. Before doing so, we highlight how this expression builds upon prior work quantifying the impacts of climate change.

Climate change will influence mortality risk $f = f(\boldsymbol{b}, \boldsymbol{c})$ through two pathways. First, a change in $\boldsymbol{C}$ will directly alter realized weather draws, changing $\boldsymbol{c}$. Second, as implied by Equation 1, a change in $\boldsymbol{C}$ will alter individuals' beliefs about their distribution of potential weather realizations, shifting how they act, and ultimately changing the optimal endogenous choice of $\boldsymbol{b}^*$. Therefore, since the climate $\boldsymbol{C}$ influences both $\boldsymbol{c}$ and $\boldsymbol{b}^*$, the probability of death at the initial time period $t = 1$ is:

$$\Pr(\text{death} \mid \boldsymbol{C}_1) = f(\boldsymbol{b}^*(Y_1, \boldsymbol{C}_1), \boldsymbol{c}(\boldsymbol{C}_1)) \tag{2}$$

Many previous empirical estimates of the effects of climate assume no adaptation takes place (e.g., Deschênes and Greenstone, 2007; Hsiang et al., 2017), such that projections of future impacts are computed assuming economic decisions embodied by $\boldsymbol{b}$ do not change. In reality, optimizing agents will update their behaviors and technologies $\boldsymbol{b}$ to attenuate climate-induced increases in mortality risk. Several analyses have empirically confirmed that accounting for endogenous changes to technology, behavior, and investment mitigates the direct effects of climate in a variety of contexts (e.g., Barreca et al., 2016; Park et al., 2020).[12] However, existing climate change projections accounting for these adaptation benefits do not account for the *costs* of adaptation, i.e., $A(\boldsymbol{b})$.

A full measure of the economic burden of climate change must account not only for the benefits

[11] The specification in Equation 1 imposes the assumption that there are no direct utility benefits or costs of adaptation behaviors or investments $\boldsymbol{b}$. In an alternative specification detailed in Appendix A.4, we allow agents to derive utility both from x and from the choice variables in $\boldsymbol{b}$; for example, air conditioning may increase utility directly, in addition to lowering mortality risk. We show that under this alternative framework, the costs of adapting to climate change that we can empirically recover include pecuniary expenditures on adaptation, $A(\boldsymbol{b})$, *net* of any changes in direct utility benefits or costs. All other aspects of the framework presented here are unaffected. Additionally, in a variant of this model in which agents derive utility directly from the climate, the interpretation of empirically recovered adaptation costs is modified to include an additional component representing changes in utility derived directly from the changing climate. However, this change of interpretation to include another term that is "netted out" in estimated adaptation costs is the only implication of adding climate directly to the utility function.

[12] For additional examples, see Schlenker and Roberts (2009); Hsiang and Narita (2012); Hsiang and Jina (2014); Barreca et al. (2015); Heutel, Miller, and Molitor (2017); Burgess et al. (2017); Auffhammer (2018a).

generated by adaptive reactions to these changes but also their cost. Thus, the total cost of changing mortality risks that result from climate change between time periods $t = 1$ and $t = 2$ is:

$$\textit{full value of mortality risk due to climate change} = VSL_2 \underbrace{[f(\boldsymbol{b}^*(Y_2, \boldsymbol{C}_2), \boldsymbol{c}(\boldsymbol{C}_2)) - f(\boldsymbol{b}^*(Y_2, \boldsymbol{C}_1), \boldsymbol{c}(\boldsymbol{C}_1))]}_{\text{observable change in mortality rate}} + \underbrace{A(\boldsymbol{b}^*(Y_2, \boldsymbol{C}_2)) - A(\boldsymbol{b}^*(Y_2, \boldsymbol{C}_1))}_{\text{adaptation costs}}, \tag{3}$$

where VSL_2 is the value of a statistical life in time period 2, or the willingness to pay for a marginal increase in the probability of survival, and is used to convert mortality risk to dollar value (Becker, 2007). Importantly, this definition includes changes in mortality risk and adaptation costs due *only* to changes in the climate, as income Y is held fixed at its $t = 2$ level. This ensures, for example, that increases in air conditioning prevalence due to rising incomes are not included in adaptation benefits or costs of climate change. Note that the omission of the costs of adaptation, $A(\boldsymbol{b})$, would underestimate the overall economic burden of warming.

The first key objective of this paper is to empirically quantify the total costs of climate change impacts on mortality risk, following Equation 3. However, the changes in adaptation costs between time periods (second term in Equation 3) are unobservable, practically speaking. In principle, data on each adaptive action could be gathered and modeled (Deschênes and Greenstone, 2011, e.g.,), but since there exists an enormous number of possible adaptive margins that together make up the composite good $\boldsymbol{b}$, computing the full cost of climate change using such an enumerative approach quickly becomes intractable.

To circumvent this challenge, we use a revealed preference approach derived from the first order conditions of the agents' problem (Equation 1) to construct empirical estimates of changes in adaptation costs due to climate change. We begin by rearranging the agent's first order conditions and using the conventional definition of the VSL (i.e., $\frac{u(x)}{[1-\tilde{f}(\boldsymbol{b},\boldsymbol{C})]\partial u/\partial x}$ (Becker, 2007)) to show that in any time period t,

$$\frac{\partial A(\boldsymbol{b}_t^*)}{\partial \boldsymbol{b}} = \frac{-u(x_t^*)}{\partial u/\partial x[1 - \tilde{f}(\boldsymbol{b}_t^*, \boldsymbol{C}_t)]} \frac{\partial \tilde{f}(\boldsymbol{b}_t^*, \boldsymbol{C}_t)}{\partial \boldsymbol{b}} = -VSL_t \frac{\partial \tilde{f}(\boldsymbol{b}_t^*, \boldsymbol{C}_t)}{\partial \boldsymbol{b}} \tag{4}$$

That is, marginal adaptation costs (lefthand side) equal the value of marginal adaptation benefits (righthand side), when evaluated at the optimal level of adaptation $\boldsymbol{b}^*$ and consumption x^*. This expression enables us to use estimates of marginal adaptation benefits infer estimates of marginal adaptation costs.

To make the expression in Equation 4 of greater practical value, we note that the total derivative of expected mortality risk with respect to a change in the climate is the sum of two terms:

$$\frac{d\tilde{f}(\boldsymbol{b}_t^*, \boldsymbol{C}_t)}{d\boldsymbol{C}} = \frac{\partial \tilde{f}(\boldsymbol{b}_t^*, \boldsymbol{C}_t)}{\partial \boldsymbol{b}} \frac{\partial \boldsymbol{b}_t^*}{\partial \boldsymbol{C}} + \frac{\partial \tilde{f}(\boldsymbol{b}_t^*, \boldsymbol{C}_t)}{\partial \boldsymbol{C}} \tag{5}$$

The first term on the righthand side of Equation 5 represents the expected impacts on mortality of all changes in adaptive investments induced by the change in climate; as discussed, this is of limited

practical value because of data and estimation limitations.[13] The second term is the direct effect that the climate would have if individuals did not adapt (i.e., the partial derivative).[14] For example, if climate change produces an increase in the frequency of heat events that threaten human health, it would be natural to expect the first term to be negative, as people make adjustments that save lives, and the second term to be positive, reflecting the impacts of heat on fatalities absent those adjustment. Equation 5 makes clear that we can express the unobservable mortality benefits of adaptation (i.e., $\frac{\partial \tilde{f}(\boldsymbol{b}_t^*, \boldsymbol{C}_t)}{\partial \boldsymbol{b}} \frac{\partial \boldsymbol{b}_t^*}{\partial \boldsymbol{C}}$) as the difference between the total and partial derivatives of the expected probability of death with respect to climate.

We use this fact in combination with Equation 4 to develop an expression for the *total* adaptation costs incurred as the climate changes gradually from $t = 1$ to $t = 2$, which is composed of elements which can be estimated:[15]

$$A(\boldsymbol{b}^*(Y_2, \boldsymbol{C}_2)) - A(\boldsymbol{b}^*(Y_2, \boldsymbol{C}_1)) = \int_1^2 \frac{\partial A(\boldsymbol{b}_t^*)}{\partial \boldsymbol{b}} \frac{\partial \boldsymbol{b}_t^*}{\partial \boldsymbol{C}} \frac{d\boldsymbol{C}_t}{dt} dt = -\int_1^2 VSL_t \left[\frac{d\tilde{f}(\boldsymbol{b}_t^*, \boldsymbol{C}_t)}{d\boldsymbol{C}} - \frac{\partial \tilde{f}(\boldsymbol{b}_t^*, \boldsymbol{C}_t)}{\partial \boldsymbol{C}} \right] \frac{d\boldsymbol{C}_t}{dt} dt \tag{6}$$

The practical value of Equation 6 is that it outlines how we can use estimates of the total and partial derivatives of mortality risk—with respect to the climate—to infer net adaptation costs, even though adaptation itself is not directly observable. In the following sections, we develop an empirical panel model exploiting both short-run and long-run variation in temperature through which the total derivative $\frac{d\tilde{f}}{d\boldsymbol{C}}$ can be separated from the partial derivative $\frac{\partial \tilde{f}}{\partial \boldsymbol{C}}$. The details of implementing Equation 6 are discussed in Section 4.5 and we empirically quantify these values globally in Section 5.3.

Before proceeding, a few details are worth underscoring. First, while we integrate over changes in climate in Equation 6, we hold income fixed at its endpoint value. This is because the goal is to develop an estimate of the additional adaptation expenditures incurred due to the changing climate only. In contrast, changes in expenditures due to rising income will alter mortality risk under climate change, but are not a consequence of the changing climate; therefore not included in our calculation of the total mortality-related costs of climate change.

Second, the revealed preference approach for recovering adaptation costs relies on the first order condition that guarantees that *marginal* costs of adaptation are equal to *marginal* benefits at the optimal choice $\{x^*, \boldsymbol{b}^*\}$. Since we can estimate marginal benefits, we can back out marginal costs.

Third, the *total* adaptation costs associated with the climate shifting from $\boldsymbol{C}_1$ to $\boldsymbol{C}_2$ are calculated by integrating marginal benefits of adaptation for a series of infinitesimal changes in climate (Equation 6), where marginal benefits continually evolve with the changing climate $\boldsymbol{C}$. Thus, total adaptation costs in a given period, relative to a base period, are the sum of the adaptation costs induced by a series of small changes in climate in the preceding periods (see Appendix A.1 for a visual description).

Finally, the *total* adaptation benefits associated with the climate shifting from $\boldsymbol{C}_1$ to $\boldsymbol{C}_2$ are defined as the dollar value of the difference between the effects of climate change with optimal adaptation and

[13] This term is often known in the environmental health literature as the effect of "defensive behaviors" (Deschênes, Greenstone, and Shapiro, 2017) and in the climate change literature as "belief effects" (Deryugina and Hsiang, 2017); in our context these effects result from changes in individuals' defensive behaviors undertaken because their beliefs about the climate have changed.

[14] This term is known in the climate change literature as the "direct effect" of the climate (Deryugina and Hsiang, 2017).

[15] Note that x is fully determined by $\boldsymbol{b}$ and income Y through the budget constraint.

without any adaptation: $-VSL_2[\tilde{f}(\boldsymbol{b}^*(Y_2, \boldsymbol{C}_2), \boldsymbol{C}_2) - \tilde{f}(\boldsymbol{b}^*(Y_2, \boldsymbol{C}_1), \boldsymbol{C}_2)]$. In contrast to total adaptation costs, this expression relies on the relationship between mortality and temperature that holds *only* at the final climate, $\boldsymbol{C}_2$. Therefore, when the marginal benefits of adaptation are greater at the final climate than at previous climates, the total benefits of adaptation will exceed total adaptation costs, generating an adaptation "surplus". For example, at a climate between $\boldsymbol{C}_1$ and $\boldsymbol{C}_2$, the marginal unit of air conditioning (a key form of adaptation) purchased will have benefits that are exactly equal to its costs. However, at the warmer climate $\boldsymbol{C}_2$, this same unit of air conditioning becomes inframarginal, and may have benefits that exceed its costs. Appendix A.2 derives a formal expression for this adaptation surplus.

2.3 The mortality partial social cost of carbon

The second objective of this paper is to quantify the mortality partial SCC. Here, we use the representative agent's problem in Equation 1 to derive an expression for the partial SCC, which we empirically estimate using a procedure outlined in Section 6.

Given the agent's expectations of the weather, the indirect utility function for the problem in Equation 1 in each period t is:

$$v_t(Y_t, A(\boldsymbol{b}_t^*), \boldsymbol{C}_t) = u(x_t^*)\left[1 - \tilde{f}(\boldsymbol{b}_t^*, \boldsymbol{C}_t)\right] + \lambda_t[Y_t - x_t^* - A(\boldsymbol{b}_t^*)], \tag{7}$$

where, as above, climate is determined by the prior evolution of global emissions through $\boldsymbol{C}_t = \varphi(E_0, E_1, E_2, ...E_t)$ and λ_t is the marginal utility of income. The mortality partial SCC is defined as the marginal willingness-to-pay (MWTP) in period t to avoid the mortality consequences from a marginal increase in emissions. Because emissions released in period t influence the trajectory of global emissions for hundreds of years (see Figure 1), this MWTP includes impacts of carbon emissions on utility in future time periods $s > t$. Thus, we derive the MWTP to avoid a marginal change in emissions in period t by differentiating the indirect utility function in each future period s with respect to emissions E_t, and integrating over time:[16]

$$\begin{aligned} \textit{Mortality partial } SCC_t \text{ (utils)} &= \int_t^\infty e^{-\delta(s-t)} \frac{-dv_s}{dE_t} ds \\ &= \underbrace{\int_t^\infty e^{-\delta(s-t)} u(x_s^*) \left(\frac{\partial \tilde{f}_s}{\partial \boldsymbol{b}} \frac{\partial \boldsymbol{b}_s^*}{\partial \boldsymbol{C}} + \frac{\partial \tilde{f}_s}{\partial \boldsymbol{C}} \right) \frac{\partial \boldsymbol{C}_s}{\partial E_t} ds}_{\substack{\text{discounted damages of emissions from} \\ \text{change in mortality rates}}} + \underbrace{\int_t^\infty e^{-\delta(s-t)} \lambda_s \frac{\partial A_s}{\partial \boldsymbol{b}} \frac{\partial \boldsymbol{b}_s^*}{\partial \boldsymbol{C}} \frac{\partial \boldsymbol{C}_s}{\partial E_t} ds}_{\substack{\text{discounted damages of emissions} \\ \text{from adaptation costs}}}, \end{aligned} \tag{8}$$

where δ indicates the discount rate.[17]

The two terms in Equation 8 show that increases in emissions cause damages through two channels. First, emissions change mortality rates, net of optimal adaptation, for all future time periods. Second,

[16] For display purposes only we have omitted the arguments of $\tilde{f}(\cdot)$ in Equations 8 and 9.

[17] Equation 8 assumes a constant discount rate δ. This approach is taken because it is standard in policy applications of the SCC (Interagency Working Group on Social Cost of Carbon, 2010), although future work should explore the implications of more complex discounting procedures, such as declining discount rates (e.g., Newell and Pizer, 2004; Millner and Heal, 2018).

emissions change the expenditures that the agent must incur in order to update her optimal adaptation.

Some manipulation allows us to convert Equation 8 into dollars. Using the standard definition of the VSL and the first order conditions from Equation 1, we divide Equation 8 by $[1 - \tilde{f}]\partial u/\partial x$ to rewrite the mortality partial SCC in units of dollars:

$$\begin{aligned} \textit{Mortality partial } SCC_t \text{ (dollars)} &= \int_t^{\infty} e^{-\delta(s-t)} \underbrace{\left[VSL_s \left(\frac{\partial \tilde{f}_s}{\partial \boldsymbol{b}} \frac{\partial \boldsymbol{b}_s^*}{\partial \boldsymbol{C}} + \frac{\partial \tilde{f}_s}{\partial \boldsymbol{C}} \right) + \frac{\partial A_s}{\partial \boldsymbol{b}} \frac{\partial \boldsymbol{b}_s^*}{\partial \boldsymbol{C}} \right]}_{\substack{\text{total monetized mortality-related damages} \\ \text{from a marginal change in climate}}} \frac{\partial \boldsymbol{C}_s}{\partial E_t} ds \\ &= \int_t^{\infty} e^{-\delta(s-t)} \frac{dD(\boldsymbol{C}_s, s)}{d\boldsymbol{C}} \frac{\partial \boldsymbol{C}_s}{\partial E_t} ds, \end{aligned} \tag{9}$$

where $D(\boldsymbol{C}_s, s)$ represents a damage function describing *total* global economic losses due to changes in mortality risk in year s, as a function of the global climate $\boldsymbol{C}$. Critically, this damage function is inclusive of adaptation benefits and costs.

In practice, we approximate Equation 9 by combining empirically-grounded estimated damage functions $D(\cdot)$ with climate model simulations of the impact of a small change in emissions on the global climate, i.e., $\frac{\partial \boldsymbol{C}_s}{\partial E_t}$. Expressing the mortality partial SCC using a damage function has three key practical advantages. First, the damage function represents a parsimonious, reduced-form description of the otherwise complex dependence of global economic damage on the global climate. Second, as we demonstrate below in Section 6, it is possible to empirically estimate damage functions from the climate change projections described in Section 2.2. Finally, because they are fully differentiable, empirical damage functions can be used to compute *marginal* costs of an emissions impulse released in year t by differentiation. The construction of these damage functions, as well as the implementation of the entire mortality partial SCC, are detailed in Section 6.

3 Data

We believe that we have collected the most comprehensive data file ever compiled on mortality, historical climate data, and climate, population, and income projections. Section 3.1 describes the data necessary to estimate the relationship between mortality and temperature. Section 3.2 outlines the data we use to predict the mortality-temperature relationship across the entire planet today and project its evolution into the future as populations adapt to climate change. Appendix B provides a more extensive description of all of these datasets.

3.1 Data to estimate the mortality-temperature relationship

Mortality data. Our mortality data are collected independently from 41 countries.[18] Combined, this dataset covers mortality outcomes for 55% of the global population, representing a substantial increase in coverage relative to existing literature; prior studies investigate an individual country (e.g., Burgess et al., 2017) or region (e.g., Deschenes, 2018), or combine small nonrandom samples from

[18] Our main analysis uses age-specific mortality rates from 40 of these countries. We use data from India as cross-validation of our main results, as the India data do not have records of age-specific mortality rates. The omission of India from our main regressions lowers our data coverage to 38% of the global population.

across multiple countries (e.g., Gasparrini et al., 2015). Spatial coverage, resolution, and temporal coverage are shown in Figure 2A, and each dataset is summarized in Table 1 and detailed in Appendix B.1. We harmonize all records into a single multi-country panel dataset of age-specific annual mortality rates, using three age categories: <5, 5-64, and >64, where the unit of observation is ADM2 (e.g., a county in the U.S.) by year. Note that the India mortality data lacks age-specific rates, and therefore is used for out-of-sample tests rather than in the main analysis.

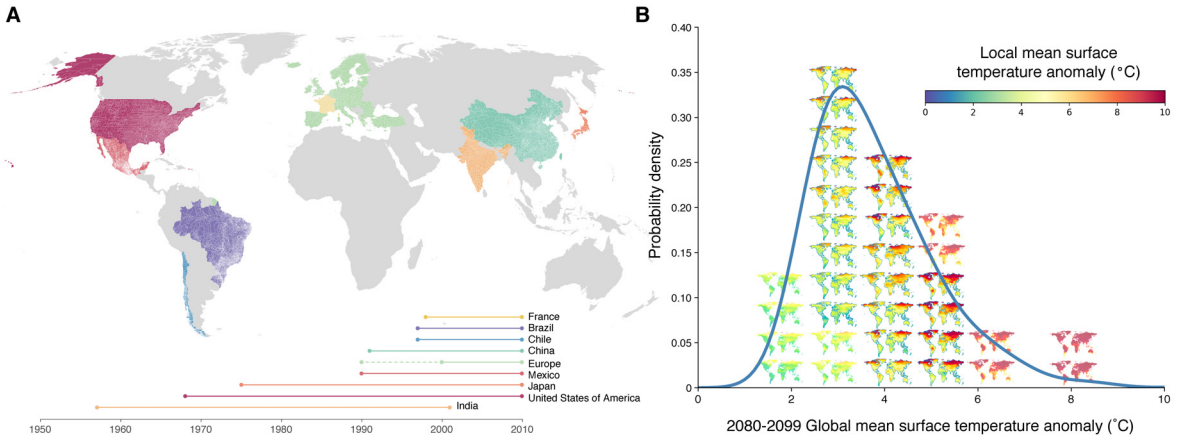

Figure 2: Mortality statistics and future climate projections used in generating empirically-based climate change mortality impact projections. Panel A shows the spatial distribution and resolution of mortality statistics from all countries used to generate regression estimates of the temperature-mortality relationship. Temporal coverage for each country is shown under the map (the dotted line for the European Union (EU) time series indicates that start dates vary for a small subset of countries). Panel B shows the 21 climate models (outlined maps) and 12 model surrogates (maps without outlines) that are weighted in climate change projections so that the weighted distribution of the 2080 to 2099 global mean surface temperature anomaly (ΔGMST) exhibited by the 33 total models matches the probability distribution of estimated ΔGMST responses (blue-gray line) under RCP8.5. For this construction, the anomaly is relative to values in 1986-2005.

Historical climate data. We perform analyses with two separate groups of historical data on precipitation and temperature. First, we use the Global Meteorological Forcing Dataset (GMFD) (Sheffield, Goteti, and Wood, 2006), which relies on a weather model in combination with observational data. Second, we repeat our analysis with climate datasets that strictly interpolate observational data across space onto grids, combining temperature data from the daily Berkeley Earth Surface Temperature dataset (BEST) (Rohde et al., 2013) with precipitation data from the monthly University of Delaware dataset (UDEL) (Matsuura and Willmott, 2007). Table 1 summarizes these data; full data descriptions are provided in Appendix B.2. We link climate and mortality data by aggregating gridded daily temperature data to the annual measures at the same administrative level as the mortality records using a procedure detailed in Appendix B.2.4 that preserves potential nonlinearities in the mortality-temperature relationship.

Covariate data. Our analysis allows for heterogeneity in the age-specific mortality-temperature relationship as a function of two long-run covariates: a measure of climate (in our main specification, long-run average temperature) and income per capita. We assemble time-invariant measures of both these variables at the ADM1 unit (e.g., state) level using GMFD climate data and a combination of the Penn World Tables (PWT), Gennaioli et al. (2014), and Eurostat (2013). The construction of the income variable requires some estimation to downscale to ADM1 level; details on this procedure are

Mortality records

Country	N	Spatial scale[×]	Years	Age categories	Average annual mortality rate[*†] All-age	Average annual mortality rate[*†] >64 yr.	Global pop. share[◇]	Average covariate values[*□] GDP per capita[⊗]	Avg. daily temp.[⊘]	Annual avg. days $> 28°C$
Brazil	228,762	ADM2	1997-2010	<5, 5-64, >64	525	4,096	0.028	11,192	23.8	35.2
Chile	14,238	ADM2	1997-2010	<5, 5-64, >64	554	4,178	0.002	14,578	14.3	0
China	7,488	ADM2	1991-2010	<5, 5-64, >64	635	7,507	0.193	4,875	15.1	25.2
EU	13,013	NUTS2[‡]	1990[▷]-2010	<5, 5-64, >64	1,014	5,243	0.063	22,941	11.2	1.6
France[⊕]	3,744	ADM2	1998-2010	0-19, 20-64, >64	961	3,576	0.009	31,432	11.9	0.3
India[^]	12,505	ADM2	1957-2001	All-age	724	–	0.178	1,355	25.8	131.4
Japan	5,076	ADM1	1975-2010	<5, 5-64, >64	788	4,135	0.018	23,241	14.3	8.3
Mexico	146,835	ADM2	1990-2010	<5, 5-64,>64	561	4,241	0.017	16,518	19.1	24.6
USA	401,542	ADM2	1968-2010	<5, 5-64, >64	1,011	5,251	0.045	30,718	13	9.5
All Countries	**833,203**	–	–	–	**780**	**4,736**	**0.554**	**20,590**	**15.5**	**32.6**

Historical climate datasets

Dataset	Citation	Method	Resolution	Variable	Source
GMFD, V1	Sheffield, Goteti, and Wood (2006)	Reanalysis & Interpolation	0.25°	temp. & precip.	Princeton University
BEST	Rohde et al. (2013)	Interpolation	1°	temp.	Berkeley Earth
UDEL	Matsuura and Willmott (2007)	Interpolation	0.5°	precip.	University of Delaware

Table 1: Historical mortality & climate data

[*] In units of deaths per 100,000 population.
[†] To remove outliers, particularly in low-population regions, we winsorize the mortality rate at the 1% level at high end of the distribution across administrative regions, separately for each country.
[□] All covariate values shown are averages over the years in each country sample.
[×] ADM2 refers to the second administrative level (e.g., county), while ADM1 refers to the first administrative level (e.g., state). NUTS2 refers to the Nomenclature of Territorial Units for Statistics 2^{nd} (NUTS2) level, which is specific to the European Union (EU) and falls between first and second administrative levels.
[◇] Global population share for each country in our sample is shown for the year 2010.
[⊗] GDP per capita values shown are in constant 2005 dollars purchasing power parity (PPP).
[⊘] Average daily temperature and annual average of the number of days above 28°C are both population weighted, using population values from 2010.
[‡] EU data for 33 countries were obtained from a single source. Detailed description of the countries within this region is presented in Appendix B.1.
[▷] Most countries in the EU data have records beginning in the year 1990, but start dates vary for a small subset of countries. See Appendix B.1 and Table B.1 for details.
[⊕] We separate France from the rest of the EU, as higher resolution mortality data are publicly available for France.
[^] It is widely believed that data from India understate mortality rates due to incomplete registration of deaths.

provided in Appendix B.3.

3.2 Data for projecting the mortality-temperature relationship around the world & into the future

Unit of analysis for projections. We partition the global land surface into a set of 24,378 regions onto which we generate location-specific projected damages of climate change. These regions (hereafter, *impact regions*) are constructed such that they are either identical to, or are a union of, existing administrative regions. They (i) respect national borders, (ii) are roughly equal in population across regions, and (iii) display approximately homogenous within-region climatic conditions. Appendix C details the algorithm used to create impact regions.

Climate projections. We use a set of 21 high-resolution bias-corrected, downscaled global climate projections produced by NASA Earth Exchange (NEX) (Thrasher et al., 2012)[19] that provide daily

[19] The dataset we use, called the NEX-GDDP, downscales global climate model (GCM) output from the Coupled

temperature and precipitation through the year 2100.[20] We obtain climate projections based on two standardized emissions scenarios: Representative Concentration Pathways 4.5 (RCP4.5, an emissions stabilization scenario) and 8.5 (RCP8.5, a scenario with intensive growth in fossil fuel emissions) (Van Vuuren et al., 2011; Thomson et al., 2011)).

These 21 climate models systematically underestimate tail risks of future climate change (Tebaldi and Knutti, 2007; Rasmussen, Meinshausen, and Kopp, 2016).[21] To correct for this, we follow Hsiang et al. (2017) by assigning probabilistic weights to climate projections and use 12 surrogate models that describe local climate outcomes in the tails of the climate sensitivity distribution (Rasmussen, Meinshausen, and Kopp, 2016). Figure 2B shows the resulting weighted climate model distribution. The 21 models and 12 surrogate models are treated identically in our calculations and we describe them collectively as the surrogate/model mixed ensemble (SMME). Gridded output from these projections are aggregated to impact regions; full details on the climate projection data are in Appendix B.2.

Socioeconomic projections. Projections of population and income are a critical ingredient in our analysis, and for these we rely on the Shared Socioeconomic Pathways (SSPs), which describe a set of plausible scenarios of socioeconomic development over the 21^{st} century (see Hsiang and Kopp (2018) for a description of these scenarios). We use SSP2, SSP3, and SSP4, which yield emissions in the absence of mitigation policy that fall between RCP4.5 and RCP8.5 in integrated assessment modeling exercises (Riahi et al., 2017). For population, we use the International Institute for Applied Systems Analysis (IIASA) SSP population projections, which provide estimates of population by age cohort at country-level in five-year increments (IIASA Energy Program, 2016). National population projections are allocated to impact regions based on current satellite-based within-country population distributions from Bright et al. (2012) (see Appendix B.3.3). Projections of national income per capita are similarly derived from the SSP scenarios, using both the IIASA projections and the Organization for Economic Co-operation and Development (OECD) Env-Growth model (Dellink et al., 2015) projections. We allocate national income per capita to impact regions using current nighttime light satellite imagery from the NOAA Defense Meteorological Satellite Program (DSMP). Appendix B.3.2 provides details on this calculation.

4 Methods

Here we describe a set of methods designed to generate future projections of the impacts of climate change on mortality across the globe, relying on empirically estimated historical relationships. In the first subsection, we detail the estimating equation used to recover the average treatment effect of temperature on mortality rates across all administrative regions in our sample. This gives us the casual estimate of temperature's impact upon mortality using historical data. In the second subsection, we describe a model of heterogeneous treatment effects that allows us to capture differences in temperature

Model Intercomparison Project Phase 5 (CMIP5) archive (Taylor, Stouffer, and Meehl, 2012), an ensemble of models typically used in national and international climate assessments.

[20] See Hsiang and Kopp (2018) for a description of climate model structure and output, as well as the RCP emissions scenarios.

[21] The underestimation of tail risks in the 21-model ensemble is for several reasons, including that these models form an ensemble of opportunity and are not designed to sample from a full distribution, they exhibit idiosyncratic biases, and have narrow tails. We are correcting for their bias and narrowness with respect to global mean surface temperature (GMST) projections, but our method does not correct for all biases.

sensitivity across distinct populations in our sample, and thus to quantify the benefits of adaptation as observed in historical data. The remaining sections detail how we combine this empirical information with the theoretical framework from Section 2 to generate global projections of mortality risk under climate change, accounting for both benefits and costs of adaptation, in addition to how we account for uncertainty in these projections.

4.1 Estimating a pooled multi-country mortality-temperature response function

We begin by estimating a pooled, multi-country mortality-temperature response function. The model exploits year-to-year variation in the distribution of daily weather to identify the response of all-cause mortality to temperature, following, for example, Deschênes and Greenstone (2011). Specifically, we estimate the following equation on the pooled mortality sample from 40 countries,[22]

$$M_{ait} = g_a(\boldsymbol{T}_{it}) + q_{ac}(\boldsymbol{R}_{it}) + \alpha_{ai} + \delta_{act} + \varepsilon_{ait} \tag{10}$$

where a indicates age category with $a \in \{< 5, 5\text{-}64, > 64\}$, i denotes the second administrative level (ADM2, e.g., county),[23] c denotes country, and t indicates years. Thus, M_{ait} is the age-specific all-cause mortality rate in ADM2 unit i in year t. α_{ai} is a fixed effect for $age \times ADM2$, and δ_{act} a vector of fixed effects that allow for shocks to mortality that vary at the $age \times country \times year$ level.

Our focus in Equation 10 is the effect of temperature on mortality, represented by the response function $g_a(\cdot)$, which varies by age. Before describing the functional form of this response, we note that our climate data are provided at the grid-cell-by-day level. To align gridded daily temperatures with annual administrative mortality records, we first take nonlinear functions of grid-level daily average temperature and sum these values across the year. This is done before the data are spatially averaged in order to accurately represent the distributions at grid cell level. We then collapse annual observations across grid cells within each ADM2 using population weights in order to represent temperature exposure for the average person within an administrative unit (see Appendix B.2.4 for details). This process results in the annual, ADM2-level vector $\boldsymbol{T}_{it}$. We then choose $g_a(\cdot)$ to be a *linear* function of the *nonlinear* elements of $\boldsymbol{T}_{it}$. This construction allows us to estimate a linear regression model while preserving the nonlinear relationship between mortality and temperature that takes place at the grid-cell-by-day level (Hsiang, 2016). The nonlinear transformations of daily temperature captured by $\boldsymbol{T}_{it}$ determine, through their linear combination in $g_a(\cdot)$, the functional form of the mortality-temperature response function.

In our main specification, $\boldsymbol{T}_{it}$ contains polynomials of daily average temperatures (up to fourth order), summed across the year. We emphasize results from the polynomial model because it strikes a balance between providing sufficient flexibility to capture important nonlinearities, parsimony, and limiting demands on the data when covariate interactions are introduced (see Section 4.2). Results for alternative functional form specifications are very similar to the fourth-order polynomial and are provided in Appendices D.1 and F. Analogous to temperature, we summarize daily grid-level precipi-

[22] We omit India in our main analysis because mortality records do not record age.

[23] This is usually the case. However, as shown in Table 1, the EU data is reported at Nomenclature of Territorial Units for Statistics 2^{nd} (NUTS2) level, and Japan reports mortality at the first administrative level.

tation in the annual ADM2-level vector $\boldsymbol{R}_{it}$. We construct $\boldsymbol{R}_{it}$ as a second-order polynomial of daily precipitation, summed across the year, and estimate an age- and country-specific linear function of this vector, represented by $q_{ac}(\cdot)$.

The core appeal of Equation 10 is that the mortality-temperature response function is identified from the plausibly random year-to-year variation in temperature within a geographic unit (Deschênes and Greenstone, 2007). Specifically, the $age \times ADM2$ fixed effects α_{ai} ensure that we isolate within-location year-to-year variation in temperature and rainfall exposure, which is as good as randomly assigned. The $age \times country \times year$ fixed effects δ_{act} account for any time-varying trends or shocks to age-specific mortality rates which are unrelated to the climate.

We fit the multi-country pooled model in Equation 10 using weighted least squares, weighting by age-specific population so that the coefficients correspond to the average person in the relevant age category and to account for the greater precision associated with mortality estimates from larger populations.[24] Standard errors are clustered at the first administrative level (ADM1, e.g., state), instead of at the unit of treatment (ADM2, e.g., county), to account for spatial as well as temporal correlation in error structure. Robustness of this model to alternative fixed effects and error structures is shown in Section 5, and to alternative climate datasets in Appendix D.1.

4.2 Heterogeneity in the mortality-temperature response function based on climate and income

The average treatment effect identified through Equation 10 is likely to mask important differences in the sensitivity of mortality rates to changes in temperature across the diverse populations included in our sample. These differences in sensitivity reflect differential investments in adaptation – i.e., different levels of $\boldsymbol{b}^*$. We cannot observe the level of $\boldsymbol{b}$ directly, but we can observe those factors that influence how poplations select an optimal $\boldsymbol{b}^*$ and condition on those directly to model heterogeneity in the temperature-mortality relationship. We develop a simple two-factor interaction model using average temperature (i.e., long-run climate) and average per capita incomes to explain cross-sectional variation in the estimated mortality-temperature relationship. This approach provides provides separate estimates for the effect of climate-driven adaptation and income growth on shape of the temperature-mortality relationship, as they are observed in the historical record.

The two factors defining this interaction model come directly from the theoretical framework in Section 2. First, a higher average temperature incentivizes investment in heat-related adaptive behaviors, as the return to any given adaptive mechanism is higher the more frequently the population experiences days with life-threatening temperatures. In Section 2, this was represented by $\boldsymbol{b}^*$ being a function of climate $\boldsymbol{C}$. In our empirical specification, we use a parsimonious parameterization of the climate, interacting our nonlinear temperature response function with the location-specific long-run average temperature.[25] Second, higher incomes relax agents' budget constraints and hence facilitate adaptive behavior. In Section 2, this was captured by optimal adaptation $\boldsymbol{b}^*$ being an implicit function

[24] We constrain population weights to sum to one for each year in the sample, across all observations. That is, our weight for an observation in region i in year t for age group a is $\omega_{it}^a = pop_{it}^a / \sum_i \sum_a pop_{it}^a$. This adjustment of weights is important in our context, as we have a very unbalanced panel, due to the merging of heterogeneous country-specific mortality datasets.

[25] In Appendix D.5, we show robustness of this parsimonious characterization of the long-run climate to a more complex specification.

of income Y. To capture this effect, we interact the temperature polynomial with location-specific per capita income.

In addition to these theoretical arguments, there is a practical reason to restrict ourselves to these two covariates when estimating this interaction model. In order to predict responses around the world and inform projections of damages in the future, it is necessary for all key covariates in the specification to be available globally today, at high spatial resolution, *and* that credible projections of their future evolution are available. Unlike other covariates that may be of interest, average incomes and climate can be extracted from the SSPs and the climate simulations, respectively. These two factors have been the focus of studies modeling heterogeneity across the broader climate-economy literature.[26]

We capture heterogeneous patterns of temperature sensitivity via the interaction model:

$$M_{ait} = g_a(\boldsymbol{T}_{it} \mid TMEAN_s, \log(GDPpc)_s) + q_{ca}(\boldsymbol{R}_{it}) + \alpha_{ai} + \delta_{act} + \varepsilon_{ait} \tag{11}$$

where s refers to ADM1-level (e.g., state or province), $TMEAN$ is the sample-period average annual temperature, $GDPpc$ is the sample-period average of annual GDP per capita, and all other variables are defined as in Equation 10. We implement a form of $g_a(\cdot)$ that exploits linear interactions between each ADM1-level covariate and all nonlinear elements of the temperature vector $\boldsymbol{T}_{it}$. The model does not include uninteracted terms for $TMEAN$ and $GDPpc$ because they are collinear with α_{ai}. In contrast to the uninteracted models in Equation 10, we estimate Equation 11 without any regression weights since we are explicitly modeling heterogeneity in treatment effects rather than integrating over it (Solon, Haider, and Wooldridge, 2015). This specification allows for the same flexibility in the functional form of temperature as in Equation 10, it is just conditional on income and climate. More details on implementation of this regression are given in Appendix D.4.[27]

Equation 11 relies on both plausibly random year-to-year fluctuations in temperature within locations and cross-sectional variation in climate and income between administrative units. We rely on cross-sectional variation to identify the interaction effects, because a representative sample of modern populations have not experienced an alternative climate that could be exploited to identify these terms. The consequence is that the case for causally interpreting the coefficients capturing interactions in Equation 11 is weaker than for other coefficients in Equation 11 and those in Equation 10.

We nonetheless view the resulting estimates as informative for at least two reasons. First, the objects of interest are the interactions, not the level of mortality, so while unobserved factors like institutions undoubtedly affect the overall mortality rate (Acemoglu, Johnson, and Robinson, 2001),

[26] See Mendelsohn, Nordhaus, and Shaw (1994); Kahn (2005); Auffhammer and Aroonruengsawat (2011); Hsiang, Meng, and Cane (2011); Graff Zivin and Neidell (2014); Moore and Lobell (2014); Davis and Gertler (2015); Heutel, Miller, and Molitor (2017); Isen, Rossin-Slater, and Walker (2017).

[27] To see how we implement Equation 11 in practice, note that in Equation 10, we estimate $g_a(\cdot)$ as the inner product between the nonlinear functions of temperature $\boldsymbol{T}_{it}$ and a vector of coefficients $\boldsymbol{\beta}_a$; that is, $g_a(\boldsymbol{T}_{it}) = \boldsymbol{\beta}_a \boldsymbol{T}_{it}$. For example, in the polynomial case, $\boldsymbol{T}_{it}$ is a vector of length P and contains the annual sum of daily average temperatures raised to the powers $p = 1, ..., P$ and aggregated across grid cells. The coefficients $\boldsymbol{\beta}_a$ therefore fully describe the age-specific nonlinear response function. In Equation 11, we allow $g_a(\boldsymbol{T}_{it})$ to change with climate and income by allowing each element of $\boldsymbol{\beta}_a$ to be a linear function of these two variables. Using this notation, our estimating equation is:

$$M_{ait} = \underbrace{(\boldsymbol{\gamma}_{0,a} + \boldsymbol{\gamma}_{1,a} TMEAN_s + \boldsymbol{\gamma}_{2,a} \log(GDPpc)_s)}_{\boldsymbol{\beta}_a} \boldsymbol{T}_{it} + q_{ca}(\boldsymbol{R}_{it}) + \alpha_{ai} + \delta_{act} + \varepsilon_{ait}$$

where $\boldsymbol{\gamma}_{0,a}, \boldsymbol{\gamma}_{1,a}$, and $\boldsymbol{\gamma}_{2,a}$ are each vectors of length P, the latter two describing the effects of $TMEAN$ and $\log(GDPpc)$ on the sensitivity of mortality M_{ait} to temperature $\boldsymbol{T}_{it}$.

their potential influence on the mortality sensitivity of temperature is less direct, particularly after adjustment for income and climate. Second, we probed the reliability of the interaction coefficients in several ways and found them to be robust. For example, we found that the estimation off Equation 11 in the main sample provides reliable estimates of the mortality temperature sensitivity in India (see Appendix section D.6), providing an out-of-sample test of Equation 11. Additionally, the coefficients are qualitatively unchanged when we use alternative characterizations of the climate (see Appendix Section D.5) and weather (see Appendix Section F).

4.3 Spatial extrapolation: Constructing a globally representative response

The fact that carbon emissions are a global pollutant requires that estimates of climate damages used to inform an SCC must be global in scope. A key challenge for generating such globally-comprehensive estimates in the case of mortality is the absence of data throughout much of the world. Often, registration of births and deaths does not occur systematically. Although we have, to the best of our knowledge, compiled the most comprehensive mortality data file ever collected, our 40 countries only account for 38% of the global population (55% if India is included, although it only contains all-age mortality rates). This leaves more than 4.2 billion people unrepresented in the sample of available data, which is especially troubling because these populations have incomes and live in climates that may differ from the parts of the world where data are available.

To achieve the global coverage essential to understanding the costs of climate change, we use the results from the estimation of Equation 11 on the observed 38% global sample to estimate the sensitivity of mortality to temperature everywhere, including the unobserved 62% of the world's population. Specifically, the results from this model enable us to use two observable characteristics – average temperature and income – to predict the mortality-temperature response function for each of our 24,378 impact regions. Importantly, it is not necessary to recover the overall mortality rate for these purposes.

To see how this is done, we note that the projected response function for any impact region r requires three ingredients. The first are the estimated coefficients $\hat{g}_a(\cdot)$ from Equation 11. The second are estimates of GDP per capita at the impact region level.[28] And third is the average annual temperature (i.e., a measure of the long-run climate) for each impact region, where we use the same temperature data that were assembled for the regressions in Equations 10 and 11.

We then predict the shape of the response function for each age group a, impact region r, and year t, up to a constant: $\hat{g}_{art} = \hat{g}_a(\boldsymbol{T}_{rt} \mid TMEAN_{rt}, \log(GDPpc)_{rt})$ for $t = 2015$. The various fixed effects in Equation 11 are unknown and omitted, since they were nuisance parameters in the original regression. This results in a unique, spatially heterogeneous, and globally comprehensive set of predicted response functions for each location on Earth.

The accuracy of the predicted response functions will depend, in part, on its ability to capture responses in regions where mortality data are unavailable. An imperfect but helpful exercise when considering whether our model is representative is to evaluate the extent of common overlap between the two samples. Figure 3A shows this overlap in 2015, where the grey squares reflect the joint distribution of GDP and climate in the full global partition of 24,378 impact regions and orange

[28] The procedure is described in Section 3.2 and Appendix B.3.2

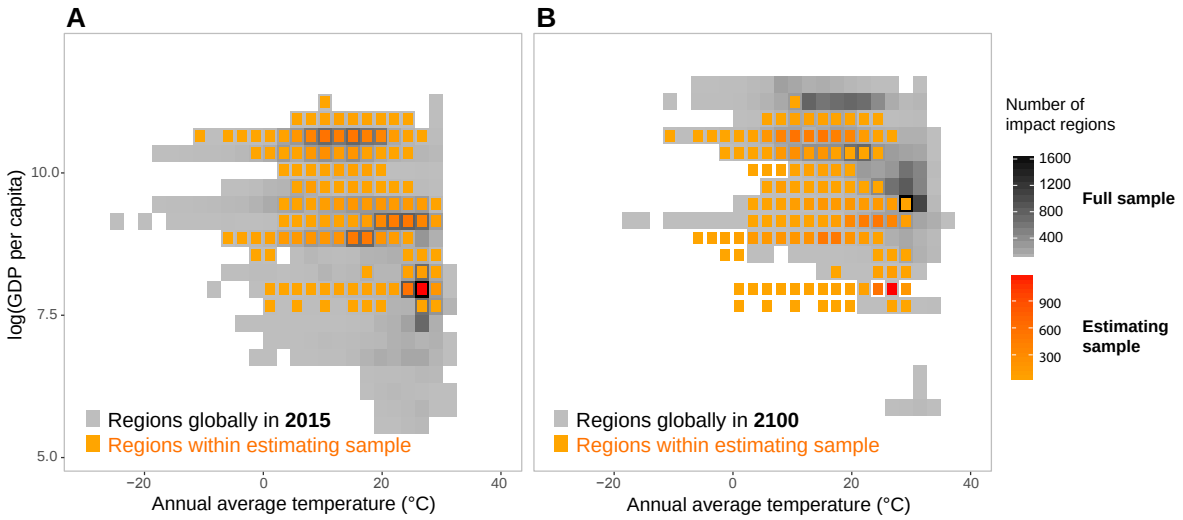

Figure 3: Joint coverage of income and long-run average temperature for estimating and full samples. Joint distribution of income and long-run average annual temperature in the estimating sample (red-orange), as compared to the global sample of impact regions (grey-black). Panel A shows in grey-black the global sample for regions in 2015. Panel B shows in grey-black the global sample for regions in 2100 under a high-emissions scenario (RCP8.5) and a median growth scenario (SSP3). In both panels, the in-sample frequency in red-orange indicates coverage for impact regions within our data sample in 2015.

squares represent the analogous distribution only for the impact regions in the sample used to estimate Equations 10 and 11. It is evident that temperatures in the global sample are generally well-covered by our data, although we lack coverage for the poorer end of the global income distribution due to the absence of mortality data in poorer countries. We explore this extrapolation to lower incomes with a set of robustness checks in Appendix D; we find the model to perform well in an out-of-sample test and to be robust to alternative functional form assumptions. We do a similar type of prediction when we project temperature-mortality relationships into the future, discussed in the next section, and thus make a similar comparison of samples. We find that, at the end of the century, the overlap is generally better, although unsurprisingly the support of our historical data does not extend to the highest projected temperatures and incomes. Thus, in our projections of the future, in some location and year combinations, we must make out-of-sample predictions about how temperature sensitivity will diminish beyond that observed anywhere in the world today, as temperatures and incomes rise outside of the support in existing global cross-section. We assess the robustness of our results to different assumptions regarding impacts of out-of-sample temperatures in Section 5.4 and Appendix F.3.

4.4 Temporal projection: Accounting for future adaptation benefits

As discussed in Section 2, a measure of the full mortality risk of climate change must account for the benefits that populations realize from optimally adapting to a gradually warming climate, as well as from income growth relaxing the budget constraint and enabling compensatory investments. Thus, we allow each impact region's mortality-temperature response function to evolve over time, reflecting how we might plausibly expect climate and incomes to change—as described in a set of internationally

standardized and widely used scenarios. We model the evolution of response functions based on projected changes to average climate and GDP per capita, again using the estimation results from fitting Equation 11.

We allow the response function in region r and in year t to evolve over time as follows. First, a 13-year moving average of income per capita in region r is calculated using national forecasts from the Shared Socioeconomics Pathways (SSP), combined with a within-country allocation of income based on present-day nighttime lights (see Appendix B.3.2), to generate a new value of $\log(GDPpc)_{rt}$. The length of this time window is chosen based on a goodness-of-fit test across alternative window lengths (see Appendix E.1). Second, a 30-year moving average of temperatures for region r is updated in each year t to generate a new level of $TMEAN_{rt}$. Finally, the response curves $\hat{g}_{art} = \hat{g}_a(\boldsymbol{T}_{rt} \mid TMEAN_{rt}, \log(GDPpc)_{rt})$ are calculated for each region for each age group in each year with these updated values of $TMEAN_{rt}$ and $\log(GDPpc)_{rt}$.

The calculation of future mortality-temperature response functions is conceptually straightforward and mirrors the procedure used to extrapolate response functions across locations that do not have historical data. However, as we are generating projections decades into the future, we must impose a set of reasonable constraints on this calculation in order to ensure plausible out-of-sample projections. The following two constraints, guided by economic theory and by the physiological literature, ensure that future response functions are consistent with the fundamental characteristics of mortality-temperature responses that we observe in the historical record and demonstrate plausible out-of-sample projections.[29] First, we impose the constraint that the response function must be weakly monotonic around an empirically estimated, location-specific, optimal mortality temperature, called the *minimum mortality temperature* (MMT). That is, we assume that temperatures farther from the MMT (either colder or hotter) must be at least as harmful as temperatures closer to the MMT. This assumption is important because Equation 11 uses within-sample variation to parameterize how the U-shaped response function flattens; with extrapolation beyond the support of historically observed income and climate, this behavior could go "beyond flat" and the response function would invert (Figure E.1). In fact, this is guaranteed to occur mechanically if enough time elapses, because our main specification only allowed income and climate to interact with the response functions linearly. However, such behavior, in which extreme temperatures are less damaging to mortality rates than more moderate temperatures, is inconsistent with a large body of epidemiological and econometric literature recovering U-shaped response functions for mortality-temperature relationships under a wide range of functional form assumptions and across diverse locations globally (Gasparrini et al., 2015; Burgess et al., 2017; Deschênes and Greenstone, 2011), as well as what we observe in our data. As a measure of its role in our results, the weak monotonicity assumption binds for the >64 age category at 35°C in 9% and 18% of impact regions in 2050 and 2100, respectively.[30] [31]

[29] See Appendix E.2 for details on these assumptions and their implementation.

[30] The frequency with which the weak monotonicity assumption binds will depend on the climate model and the emissions and socioeconomic trajectories used; reported statistics refer to the CCSM4 model under RCP8.5 with SSP3.

[31] In imposing this constraint, we hold the MMT fixed over time at its baseline level in 2015 (Figure E.1D). We do so because the use of spatial and temporal fixed effects in Equation 11 implies that response function levels are not identified; thus, while we allow the *shape* of response functions to evolve over time as incomes and climate change, we must hold fixed their *level* by centering each response function at its time-invariant MMT. Note that these fixed effects are by definition not affected by a changing weather distribution. Thus, their omission does not influence estimates of climate change impacts.

Second, we assume that rising income cannot make individuals worse off, in the sense of increasing the temperature sensitivity of mortality. Because increased income per capita strictly expands the choice set of individuals considering whether to make adaptive investments, it should not increase the effect of temperature on mortality rates. We place no restrictions on the cross-sectional effect of income on the temperature sensitivity when estimating Equation 11, but we constrain the marginal effect of income on temperature sensitivity to be weakly negative in future projections. This assumption never binds for temperature sensitivity to hot days (>35°C).[32]

Under these two constraints, we estimate projected impacts separately for each impact region and age group for each year from 2015 to 2100 by applying projected changes in the climate to these spatially and temporally heterogeneous response functions. We compute the nonlinear transformations of daily average temperature that are used in the function $g_a(\boldsymbol{T}_{rt})$ under both the RCP4.5 and RCP8.5 emissions scenarios for all 33 climate projections in the SMME (as described in Section 3.2). This distribution of climate models captures uncertainties in the climate system through 2100.

4.5 Computing adaptation costs using empirical estimates

As shown in Section 2, the full cost of the mortality risk due to climate change is the sum of the observable change in mortality and adaptation costs (Equation 3). The latter cannot be observed directly; however, as derived in Section 2.2, we can recover an expression for adaptation costs that is, in principle, empirically tractable. Specifically, these costs can be computed by taking the difference between the total and partial derivative of expected mortality risk with respect to changes in the climate, and integrating this difference (Equation 6). Here, we describe a practical implementation for this calculation.

Our empirical approximation of the adaptation costs incurred as the climate changes gradually from $t = 1$ to $t = 2$ is:

$$\begin{aligned} \widehat{A(\boldsymbol{b}^*(Y_2, \boldsymbol{C}_2)) - A}(\boldsymbol{b}^*(Y_2, \boldsymbol{C}_1)) &\approx -\int_1^2 VSL_t \left[\frac{d\hat{\tilde{f}}(\boldsymbol{b}_t^*, \boldsymbol{C}_t)}{d\boldsymbol{C}} - \frac{\partial \hat{\tilde{f}}(\boldsymbol{b}_t^*, \boldsymbol{C}_t)}{\partial \boldsymbol{C}} \right] \frac{d\boldsymbol{C}_t}{dt} dt \\ &\approx -\sum_{\tau=t_1+1}^{t_2} VSL_\tau \underbrace{\left(\frac{\partial \mathrm{E}[\hat{g}]}{\partial TMEAN}\bigg|_{\boldsymbol{C}_\tau, Y_2} \right)}_{\hat{\boldsymbol{\gamma}}_1 \mathrm{E}[\boldsymbol{T}]_\tau} (TMEAN_\tau - TMEAN_{\tau-1}), \quad (12) \end{aligned}$$

where the first line of Equation 12 is identical to Equation 6, except that we use "hat" notation to indicate that $\hat{\tilde{f}}(\cdot)$ is an empirical estimate of expected mortality risk. The second (approximate) equality follows from (i) taking the total and partial derivative of our estimating equation (Equation 11) with respect to climate — where the total derivative accounts for adaptation while the partial does not, (ii) substituting terms and simplifying the expression, and (iii) implementing a discrete-time approximation for the continuous integral (see Appendix A.3 for a full derivation). The under-braced object, $\hat{\boldsymbol{\gamma}}_1 \mathrm{E}[\boldsymbol{T}]_\tau$, is the product of the expectation of temperature and the coefficient associated

[32]The assumption that rising income cannot increase the temperature sensitivity of mortality does not bind for hot days because our estimated marginal effects of income are negative for high temperatures (see Table D.3). However, it does bind for the >64 age category under realized temperatures in 30% and 24% of impact regions days in 2050 and 2100, respectively.

with the interaction between temperature and climate from estimating equation 11: it represents our estimate of marginal adaptation benefits.[33] This derivative is then multiplied by the change in average temperature between each period.[34]

In implementation of Equation 12, we treat the VSL as a function of income, which evolves with time, but as invariant to changes in the climate (see Section 6). Note that these adaptation cost estimates are calculated for each impact region, age group, and year, using $t = 2015$ as the baseline year, for each of our 33 high-resolution climate model projections.

4.6 Accounting for uncertainty in projected mortality effects of climate change

An important feature of the analysis is to develop estimates of the mortality impacts of climate change that reflect the inherent uncertainty in these future projections.[35] As discussed in Sections 4.4 and 4.5, we construct estimates of the mortality risk of climate change for each of 33 distinct climate projections in the SMME, capturing uncertainty in the climate system.[36] Additionally, there exists an important second source of uncertainty in our projected impacts that is independent of physical uncertainty, arising from the econometric estimates of response functions; i.e., uncertainty in the estimate of $\hat{g}_a(\cdot)$.

In order to account for both of these sources of uncertainty, we execute a Monte Carlo simulation following the procedure in Hsiang et al. (2017). First, for each age category, we randomly draw a set of parameters, corresponding to the terms composing $\hat{g}_a(\cdot)$, from an empirical multivariate normal distribution characterized by the covariance between all of the parameters from the estimation of Equation 11.[37] Second, using these parameters in combination with location- and time-specific values of income and average climate provided by a given SSP scenario and RCP-specific climate projection from each of the 33 climate projections in the SMME, we construct a predicted response function for each of our 24,378 impact regions. Third, with these response functions in hand, we use daily weather realizations for each impact region from the corresponding simulation to predict an annual mortality impact. Finally, this process is repeated until approximately 1,000 projection estimates are complete for each impact region, age group, and RCP-SSP combination.

With these ∼1,000 response functions, we calculate the full mortality risk (i.e., inclusive of adaptation benefits and costs) for each impact region for each year between 1981 and 2100. The resulting calculation is computationally intensive (requiring ∼94,000 hours of CPU time across all scenarios reported in the main text and Appendix) but incorporates important uncertainty from climate and

[33] Recall that the specific functional form we use to estimate mortality risk as a function of temperature, climate, and income is $g(\cdot) = (\boldsymbol{\gamma}_0 + \boldsymbol{\gamma}_1 TMEAN_t + \boldsymbol{\gamma}_2 \log(GDPpc)_t)\,\boldsymbol{T}_t$. Thus, the partial derivative $\frac{\partial \mathrm{E}[\hat{g}]}{\partial TMEAN}$ is equivalent to $\hat{\boldsymbol{\gamma}}_1 \mathrm{E}[\boldsymbol{T}]_\tau$.

[34] We assume that individuals use the recent past to form expectations about current temperature realizations, so this expectation is computed over the prior 15 years, with weights of historical observations linearly declining in time.

[35] See Burke et al. (2015) for a discussion of combining physical uncertainty from multiple models in studies of climate change impacts.

[36] Note that while the SMME fully represents the tails of the climate sensitivity distribution as defined by a probabilistic simple climate model (see Appendix B.2.3), there remain important sources of climate uncertainty that are not captured in our projections, due to the limitations of both the simple climate model and the GCMs. These include some climate feedbacks that may amplify the increase of global mean surface temperature, as well as some factors affecting local climate that are poorly simulated by GCMs.

[37] Note that coefficients for all age groups are estimated jointly in Equation 11, such that across-age-group covariances are accounted for in this multivariate distribution.

econometric sources. When reporting projected impacts in any given year, we report summary statistics (e.g., mean, median) of this entire distribution.

5 Results I: Full mortality risk of climate change

This section presents results describing temperature's impact on mortality, heterogeneity in that impact, and projections of the full mortality risk of climate change into the future. Projections of global climate change impacts rely on extrapolation of mortality-temperature responses to parts of the world where historical mortality data are unavailable and to future time periods; applying the approaches described in Sections 4.3 and 4.4. Using the approach outlined in Sections 4.5 and 4.6, we then calculate the full global mortality risk of climate change, accounting for the benefits and costs of adaptation and for climate model and econometric uncertainty.

5.1 The mortality-temperature relationship: Pooled multi-country results

Pooling subnational mortality records across 40 countries and all age groups, we first estimate a version of Equation 10 in which $g(\boldsymbol{T}_{it})$ does not depend on age, showing results for the all-age mortality-temperature response function obtained with a fourth-order polynomial in daily average temperature. Table 2 displays this result, showing marginal effects at various temperatures. These estimates can be interpreted as the change in the number of deaths per 100,000 per year resulting from one additional day at each temperature, compared to the reference day of 20°C (68°F). Columns (1)-(3) increase the saturation of temporal controls in the model specification, ranging from country-year fixed effects in column (1) to country-year-age fixed effects in column (2) and adding age-specific state-level linear trends in column (3). Our preferred specification is column (2), as column (1) does not account for differential temporal shocks to mortality rates by age group, while in column (3) we cannot reject the null of equal age-specific, ADM1-level trends.

The data reveal the U-shaped response that is common in the prior literature across all specifications. This is a noteworthy finding because the previous literature has relied on samples with much more restrictive geographic and population coverage. Examining column (2), we find that a day at 35°C (95°F) leads to an increase in the all-age mortality rate of approximately 0.4 deaths per 100,000, relative to a day at 20°C. A day at -5°C (23°F) similarly increases the all-age mortality rate by 0.3 deaths per 100,000. This result is robust to alternative functional form assumptions (i.e., different nonlinear functions of $\boldsymbol{T}_{it}$), including a non-parametric binned regression, as well as to the use of alternative, independently-sourced, climate datasets (Figure D.1).

Age group heterogeneity. As prior work has shown that age cohorts respond differently to temperature, and because we expect considerable demographic transitions in the future, we test for heterogeneity across age groups using Equation 10. Specifically, we allow for separate mortality-temperature response functions $g_a(\boldsymbol{T}_{it})$ for each of three age categories. Figure 4 displays the mortality-temperature responses for each of our three age categories (<5, 5-64, >64) estimated from Equation 10 and using the pooled 41-country sample. These curves correspond with our primary specification (equivalent to column (2) in Table D.1).[38] This reveals substantial heterogeneity across age groups

[38]Regression results for all specifications shown in Table 2 are also shown for the age-specific model in Table D.1.

Table 2: Temperature-mortality response function estimated using pooled subnational data across 40 countries. This table shows coefficient estimates (standard errors) for a temperature-mortality response function estimated using pooled subnational data across 40 countries and 38% of the global population. Regression estimates are from a fourth-order polynomial in daily average temperature and are estimated using GMFD temperature data with a sample that was winsorized at the top 1% level. Point estimates indicate the effect of a single day at each daily average temperature value shown, relative to a day with an average temperature of 20°C (68°F).

	All-age mortality rate (per 100,000)				
	(1)	(2)	(3)	(4)	(5)
35° C	0.410***	0.446***	0.210*	0.675**	0.470***
	(0.128)	(0.168)	(0.118)	(0.274)	(0.163)
30° C	0.305***	0.307***	0.130**	0.338***	0.323***
	(0.068)	(0.080)	(0.065)	(0.106)	(0.075)
25° C	0.147***	0.141***	0.054	0.119***	0.150***
	(0.037)	(0.035)	(0.039)	(0.031)	(0.034)
20° C	–	–	–	–	–
	–	–	–	–	–
0° C	0.121	0.114	0.108	0.144**	0.070
	(0.125)	(0.128)	(0.100)	(0.067)	(0.122)
-5° C	0.307**	0.275*	0.193*	0.244**	0.212
	(0.152)	(0.158)	(0.105)	(0.096)	(0.148)
Adj R-squared	0.983	0.989	0.991	0.999	0.989
N	820697	820237	820237	820237	820237
Age × ADM2 FE	Yes	Yes	Yes	Yes	Yes
Country × Year FE	Yes				
AGE × Country × Year FE		Yes	Yes	Yes	Yes
Age × ADM1 linear trend			Yes		
Precision weighting (FGLS)				Yes	
13-month exposure					Yes

Standard errors clustered at the ADM1 (e.g., state) level.
Regressions in columns (1)-(3), and (5) are population-weighted.
Column (4) weights use a precision-weighting approach (see text).
*** p<0.01, ** p<0.05, * p<0.1

within our multi-country sample. In our preferred specification, people over the age of 64 experience approximately 4.7 extra deaths per 100,000 for a day at 35°C compared to a day at 20°C, a substantially larger effect than that for younger cohorts, which exhibit little response. This age group is also more severely affected by cold days; estimates suggest that people over the age of 64 experience 3.4 deaths per 100,000 for a day at −5°C compared to a day at 20°C, while there is a relatively weak mortality response to these cold days for other age categories. Overall, these results demonstrate that the elderly are disproportionately harmed by additional hot days and disproportionately benefit from reductions in cold days, consistent with prior evidence from the U.S. (Deschênes and Moretti, 2009; Heutel, Miller, and Molitor, 2017). It is important to note, however, that the oldest age group (over 64 years) accounts for just 12% of the population in our historical sample, causing it to differ from the average treatment effect in Table 2.

Alternative specifications. In both Tables 2 and D.1, columns (4) and (5) provide results from alternative specifications. In column (4), we address the fact that some of our data are drawn from countries which may have less capacity for data collection than others in the sample. Because our mortality data is collected by institutions in different countries, it is possible that some sources are

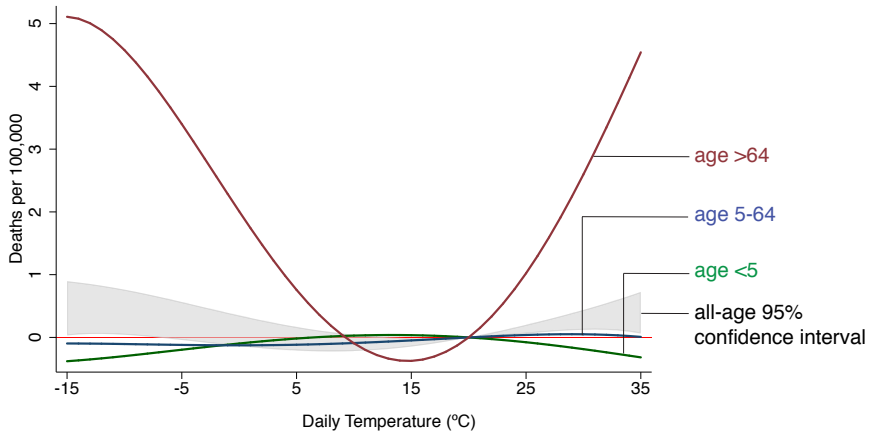

Figure 4: Mortality-temperature response function with demographic heterogeneity. Mortality-temperature response functions are estimated for populations <5 years of age (green), between 5 and 64 years of age (blue), and >64 years of age (red). Regression estimates shown are from a fourth-order polynomial in daily average temperature and are estimated using GMFD weather data with a sample that was winsorized at the 1% level. All response functions are estimated jointly in a stacked regression model that is fully saturated with age-specific fixed effects (Equation 10).

systematically less precise. To account for this, we re-estimate our model using Feasible Generalized Least Squares (FGLS) under the assumption of constant variance within each ADM1 unit.[39] In column (5), we address the possibility that temperatures can exhibit lagged effects on health and mortality (e.g., Deschênes and Moretti, 2009; Barreca et al., 2016; Guo et al., 2014). Lagged effects within and across months in the same calendar year are accounted for in the net annual mortality totals used in all specifications. However, it is possible that temperature exposure in December of each year affects mortality in January of the following year. To account for this, in column (5) we define a 13-month exposure window to additionally account for temperatures previous December.[40] Tables 2 and D.1 show that the results for both of these alternative specifications are similar in sign and magnitude to those from column (2).

5.2 Subnational heterogeneity in the mortality-temperature response

It is likely that Equation 10 obscures heterogeneity in the mortality-temperature response function; this subsection evaluates whether mortality sensitivity to temperature varies with average climate and average income through estimation of Equation 11. Tabular results are reported in Table D.3 for each of three age groups. As these terms are difficult to interpret, we visualize this heterogeneity by dividing

[39]To do this, we estimate the model in Equation 10 using population weights and our preferred specification (column (2)). Using the residuals from this regression, we calculate an ADM1-level weight that is equal to the average value of the squared residuals, where averages are taken across all ADM2-age-year level observations that fall within a given ADM1. We then inverse-weight the regression in a second stage, using this weight. All ADM2-age-year observations within a given ADM1 are assigned the same weight in the second stage, where ADM1 locations with lower residual variance are given higher weight. For some ADM2s, there are insufficient observations to identify age-specific variances; to ensure stability, we dropped the ADM2s with less than 5 observations per age group. This leads us to drop 246 (of >800,000) observations in this specification.

[40]The specification in column (5) defines the 13-month exposure window such that for a given year t, exposure is calculated as January to December temperatures in year t *and* December temperature in year $t-1$.

the sample into terciles of income and climate (i.e., the two interaction terms), creating nine discrete bins that partition the $\log(GDPpc) \times TMEAN$ space. We plot predicted response functions at the mean value of climate and income within each of these nine bins, using the coefficients in Table D.3. This results in a set of predicted response functions that vary across the joint distribution of income and average temperature within our sample data. The resulting response functions are shown in Figure 5 for the >64 age category (other age groups are shown in Appendix D.4), where average incomes are increasing across bins vertically and average temperatures are increasing across bins horizontally.

The Figure 5 results are broadly consistent with the predictions from the theoretical framework in Section 2. Recall that we expect increased frequency of exposure to higher temperatures to incentivize investment in adaptive behaviors or technologies, as the marginal mortality benefit of adaptation is higher in hotter locations. This would lead to lower temperature sensitivities to heat in places which are warmer. A striking visual finding is that within each income tercile, the effect of hot days (e.g., days >35°C) declines as one moves from left (cold climates) to right (hot climates). Similarly, a loosening of the budget constraint, as proxied by increasing GDP per capita, should enable individuals to invest further in adaptation. Indeed, Figure 5 reveals that moving from the bottom (low income) to top (high income) within a climate tercile causes a substantial flattening of the response function, especially at high temperatures.

Two statistics help to summarize the findings from Figure 5. First, in the >64 age category across all income values, moving from the coldest to the hottest tercile saves on average 7.9 (p-value=0.06) deaths per 100,000 at 35°C. Second, moving from the poorest to the richest tercile across all climate values in the sample saves approximately 5.0 (p-value=0.1) deaths per 100,000 at 35°C for the > 64 age category.

5.3 Spatial extrapolation of temperature sensitivity

Figure 6 reports on our extrapolation of mortality-temperature response functions to the entire globe. In panel A, these predicted mortality-temperature responses are plotted for each impact region for 2015 values of income and climate for the oldest age category and for the impact regions that fall within the countries in our mortality dataset ("in-sample"). Despite a shared overall shape, panel A reveals substantial heterogeneity across regions in this temperature response. Panel B shows an analogous figure for the youngest age category. Geographic heterogeneity within our sample is shown for hot days in the maps in panels C and D, where colors indicate the marginal effect of a day at 35°C day, relative to a day at a location-specific minimum mortality temperature. Grey areas are locations where mortality data are unavailable.

Figure 6E–H show analogous plots, but now extrapolated to the entire globe. We can fill in the estimated mortality effect of a 35°C day for regions without mortality data by using location-specific information on income and climate during 2015. The predicted responses at the global scale imply that a 35°C day increases the average mortality rate across the globe for the oldest age category by 10.1 deaths per 100,000 relative to a location-specific minimum mortality temperature.[41] It is important to note that the effect in locations without mortality data is 11.7 deaths per 100,000, versus 7.8 within

[41]This average impact of a 35°C is derived by taking the unweighted average level of the mortality-temperature response function evaluated at 35° across each of 24,378 impact regions globally.

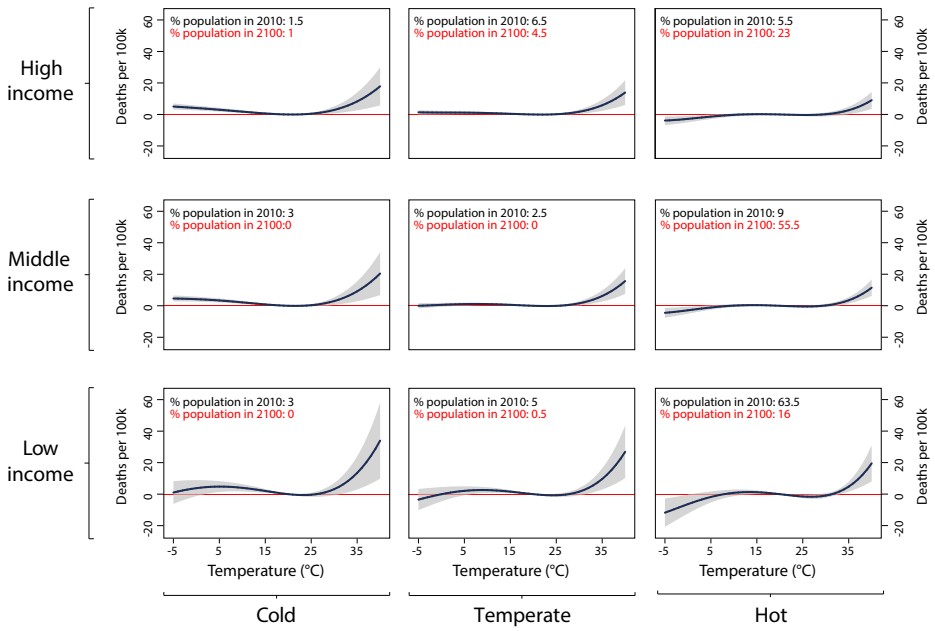

Figure 5: Heterogeneity in the mortality-temperature relationship (age >64 mortality rate). Each panel represents a predicted mortality-temperature response function for the >64 age group for a subset of the income-average temperature covariate space within our data sample. Response functions in the lower left apply to the low-income, cold regions of our sample, while those in the upper right apply to the high-income, hot regions of our sample. Regression estimates are from a fourth-order polynomial in daily average temperature and are estimated using GMFD weather data with a sample that was winsorized at the 1% level on the top end of the distribution only. All response functions are estimated jointly in a stacked regression model that is fully saturated with age-specific fixed effects, and where each temperature variable is interacted with each covariate. Values in the top left-hand corner of each panel show the percentage of the global population that reside within each tercile of average income and average temperature in 2010 (black text) and as projected in 2100 (red text, SSP3).

the sample of countries for which mortality data are available, largely driven by the fact that our sample represents wealthier populations where temperature responses are more muted. Overall, there is substantial heterogeneity across the planet and it is evident that the effects of temperature on human well-being are quite different in places where we are and are not able to obtain subnational mortality data.

5.4 Projection of future climate change impacts and adaptation

The previous subsection demonstrated that the model of heterogeneity outlined in Equation 11 allows us to extrapolate mortality-temperature relationships to regions of the world without mortality data today. However, to calculate the full global mortality risks of climate change, it is also necessary to allow these response functions to change through time to capture the benefits of adaptation and the effects of income growth. We use our model of heterogeneity and downscaled projections of income and climate to predict impact region-level response functions for each age group and year, as described in Section 4.4. Uncertainty in these estimated response functions is accounted for through Monte Carlo simulation, as described in Section 4.6. Throughout this subsection, we show results relying on income and population projections from the socioeconomic scenario SSP3; see Appendix F for results using SSP2 and SSP4. The methodology we develop to estimate future impacts of climate change

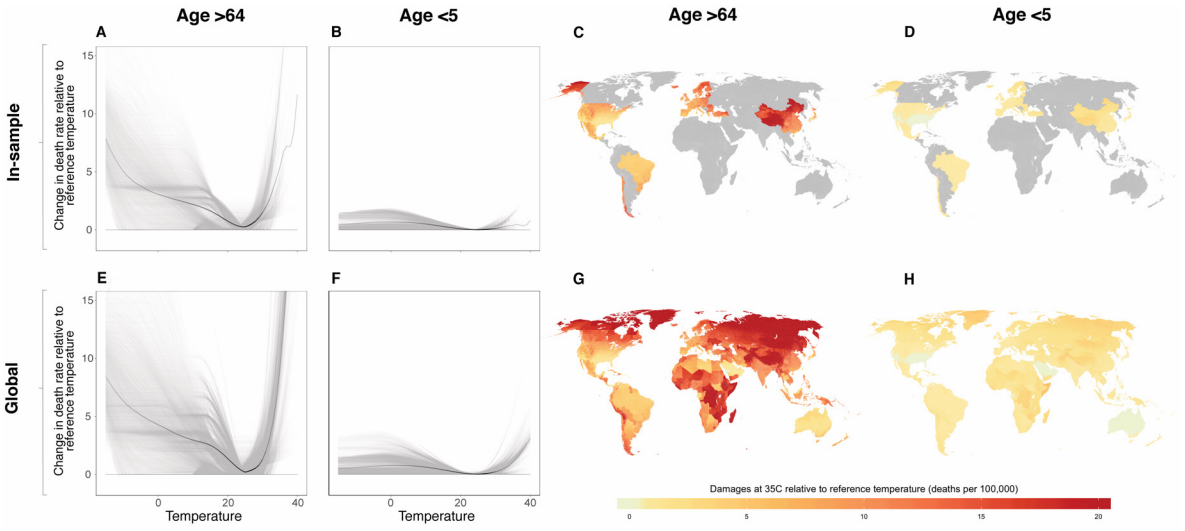

Figure 6: Using income and climate to predict current response functions globally. In panels A, B, E and F, grey lines are predicted response functions for impact regions, each representing a population of 276,000 on average. Solid black lines are the unweighted average of the grey lines, where the opacity indicates the density of realized temperatures (Hsiang, 2013). Panels C, D, G and H show each impact region's mortality sensitivity to a day at 35°C, relative to a location-specific minimum mortality temperature. The top row shows all impact regions in the sample of locations with historical mortality data (included in main regression tables), and the bottom row shows extrapolation to all impact regions globally. Column titles indicate corresponding age categories. Predictions shown are averages over the period 2001-2015.

on mortality, as well as a partial mortality-only SCC, can be applied to any available socioeconomic scenario. We show results relying on SSP3 throughout the main text because its historic global growth rates in GDP per capita and population match observed global growth rates over the 2000-2018 period much more closely than either SSP2 or SSP4 (see Table B.3 in Appendix B.3.2).

Projected adaptation benefits. Figure 7 provides an initial look into changes in the mortality-temperature relationship over time, which is a key ingredient for projections of future damages and adaptation. In particular, we plot the spatial distribution of the *change* in the mortality-temperature relationship evaluated at 35°C between 2015 and 2050 (panel A) and 2015 and 2100 (panel B) for the >64 age category.[42] The maps reveal that in most regions of the world, there is a clear downward trend in the sensitivity of mortality rates to high temperatures, as locations get both richer and hotter as the century unfolds. For the >64 age group, the average global increase in the mortality rate on a 35°C day (relative to a day at location-specific minimum mortality temperatures) declines by roughly 75% between 2015 and 2100, going from 10.1 per 100,000 to just 2.4 per 100,000 in 2100. Increasing incomes account for 77% of the decline in marginal damages for the >64 age category with adaptation to climate explaining the remainder; income gains account for 89% and 82% of the decline for the <5 and 5-64 categories, respectively.[43]

Defining four measures of expected climate change impacts. We now use our estimates of adaptation benefits, adaptation costs, and changes in climate exposure to develop measures of the

[42]Specifically, these values are $\hat{g}_a(\boldsymbol{T}|TMEAN_{r,2050}, \log(GDPpc)_{r,2050}) - \hat{g}_a(\boldsymbol{T}|TMEAN_{r,2015}, \log(GDPpc)_{r,2015})$ and $\hat{g}_a(\boldsymbol{T}|TMEAN_{r,2100}, \log(GDPpc)_{r,2100}) - \hat{g}_a(\boldsymbol{T}|TMEAN_{r,2015}, \log(GDPpc)_{r,2015})$, all evaluated at daily temperature $T = 35°\text{C}$ for age group a >64.

[43]These values apply to socioeconomic scenario SSP3.

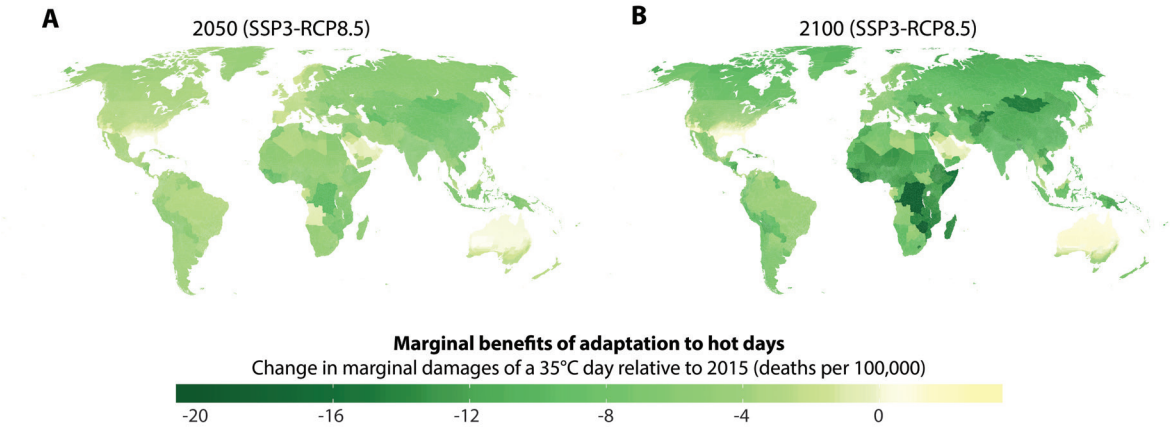

Figure 7: Spatial and temporal heterogeneity in temperature sensitivity. Panels A and B indicate the change in mortality sensitivity to hot days (35°C) for the oldest age category (>64) between 2015 and 2050 (A), and between 2015 and 2100 (B). Darker colors signify larger predicted adaptation to heat. All values shown refer to the RCP8.5 emissions scenario and the SSP3 socioeconomic scenario.

expected costs of climate change induced mortality risk. In so doing, we separate the role of income growth from that of adaptation to warming. While the central welfare metric of concern is the full mortality-related costs of climate change, i.e., the sum of the increase in deaths and adaptation costs (Equation 3), we also derive three other measures of climate change impacts that elucidate the roles of adaptation and income growth in determining the full mortality-related costs. The empirical estimation of each of these measures is first reported in units of deaths per 100,000, although it is straightforward to monetize these measures using estimates of the value of a statistical life (VSL), and we do so at the end of this section.

Note that in all expressions of climate change impacts below, the first term represents the predicted mortality rate under a future warming climate. The second term represents a counterfactual predicted mortality rate that would be realized under current temperatures, but in a population that benefits from rising incomes over the coming century. These counterfactuals thus include the prediction, for example, that air conditioning will become much more prevalent in a country like India as the economy grows, regardless of whether climate change unfolds or not. One exception is expression (i), where the counterfactual is identical to that under current temperatures and incomes, as in this case the climate change projection ignores income growth and adaptation entirely. By subtracting off these counterfactuals, our predicted changes in mortality rates isolate the additional cost of climate change on a population experiencing economic growth.

The first measure is the *mortality effects of climate change with neither adaptation nor income growth*, which provides an estimate of the increases in mortality rates when each impact region's response function in each year t is a function of their 2015 level of income and average climate. In other words, mortality sensitivity to temperature is assumed not to change with future income or temperature. This is a benchmark model often employed in previous work. Specifically, the expected climate induced mortality risk that we estimate for an impact region and age group in a future year t under this measure are (omitting subscripts for impact regions and age groups for clarity):[44]

[44]Note that in all estimates of climate change impacts in (i)–(iv), population growth is accounted for as an exogenous

(i) *Mortality effects of climate change with neither adaptation nor income growth*:

$$\underbrace{\hat{g}(\boldsymbol{T}_t \mid TMEAN_{2015}, \log(GDPpc)_{2015})}_{\substack{\text{mortality risk with climate change} \\ \text{and without adaptation}}} - \underbrace{\hat{g}(\boldsymbol{T}_{2015} \mid TMEAN_{2015}, \log(GDPpc)_{2015})}_{\text{current mortality risk}}$$

The second measure is the *mortality effects of climate change with benefits of income growth*, which allows response functions to change with future incomes. This measure captures the change in mortality rates that would be expected from climate change if populations became richer, but they did not respond optimally to warming by adapting above and beyond how they would otherwise cope with their historical climate. This measure is defined as:

(ii) *Mortality effects of climate change with benefits of income growth*:

$$\underbrace{\hat{g}(\boldsymbol{T}_t \mid TMEAN_{2015}, \log(GDPpc)_t)}_{\substack{\text{mortality risk with benefits of income growth} \\ \text{and climate change}}} - \underbrace{\hat{g}(\boldsymbol{T}_{2015} \mid TMEAN_{2015}, \log(GDPpc)_t)}_{\substack{\text{mortality risk with benefits of income growth,} \\ \text{without climate change}}}$$

The third measure is the *mortality effects of climate change with benefits of income growth and adaptation*, and in this case populations adjust to experienced temperatures in the warming scenario. This metric is an estimate of the observable deaths that would be expected under a warming climate, accounting for the benefits of optimal adaptation and income growth:

(iii) *Mortality effects of climate change with benefits of income growth and adaptation*:

$$\underbrace{\hat{g}(\boldsymbol{T}_t \mid TMEAN_t, \log(GDPpc)_t)}_{\substack{\text{mortality risk with benefits of income growth} \\ \text{and adaptation to climate change}}} - \underbrace{\hat{g}(\boldsymbol{T}_{2015} \mid TMEAN_{2015}, \log(GDPpc)_t)}_{\substack{\text{mortality risk with benefits of income growth,} \\ \text{without climate change}}}$$

The final measure is the most complete, as it captures both the benefits and costs of adaptation. Recall that adaptation costs cannot be observed directly, but that we construct estimates using the revealed preference methodology detailed in Section 2. We call this measure the *full mortality risk of climate change*, and it captures the opportunity costs of investing in the adaptation benefits described by (iii):

(iv) *Full mortality risk of climate change* (including adaptation costs, recall Equation 3):

$$\underbrace{\hat{g}(\boldsymbol{T}_t \mid TMEAN_t, \log(GDPpc)_t) - \hat{g}(\boldsymbol{T}_{2015} \mid TMEAN_{2015}, \log(GDPpc)_t)}_{\text{mortality effects of climate change with benefits of income growth and adaptation (iii)}} + \underbrace{\frac{1}{VSL}\left[A(TMEAN_t, GDPpc_t) - \widehat{A(TMEAN_{2015}, GDPpc_t)}\right]}_{\text{estimated adaptation costs}}$$

In all of these measures, year $t = 2015$ is treated as the baseline year, meaning that climate change impacts are defined to be zero in this year. These four measures are all reported below in units of

projection that does not depend on the climate.

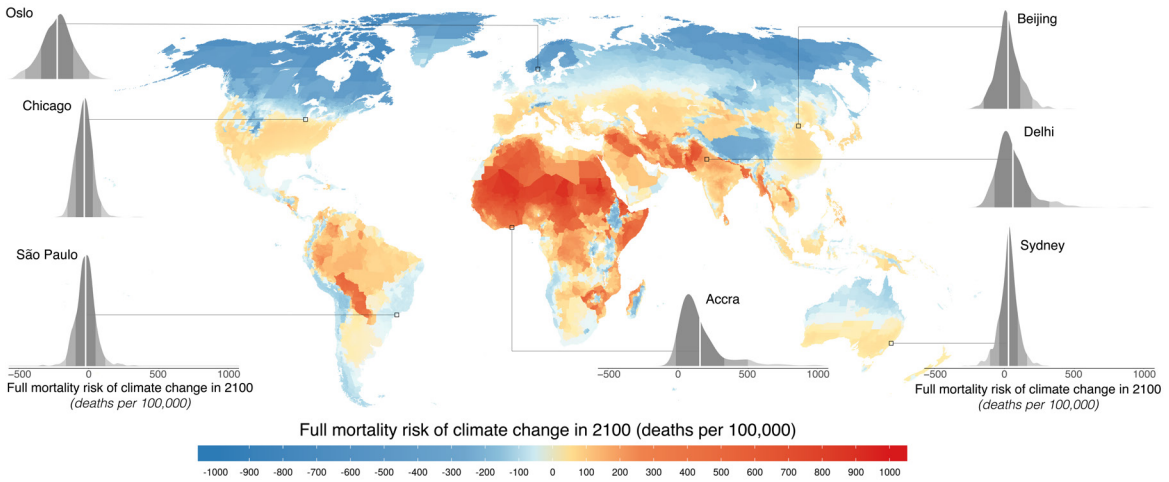

Figure 8: The mortality risk of future climate change. The map indicates the full mortality risk of climate change, measured in units of deaths per 100,000 population, in the year 2100. Estimates come from a model accounting for both the costs and the benefits of adaptation, and the map shows the climate model weighted mean estimate across Monte Carlo simulations conducted on 33 climate models; density plots for select regions indicate the full distribution of estimated impacts across all Monte Carlo simulations. In each density plot, solid white lines indicate the mean estimate shown on the map, while shading indicates one, two, and three standard deviations from the mean. All values shown refer to the RCP8.5 emissions scenario and the SSP3 socioeconomic scenario. See Figure F.4 for a comparison of impacts to RCP4.5 and SSP3

human lives. Using human lives serves as a natural numeraire in this revealed preference framework since we estimate adaptation costs based on lives that could be saved via adaptation, but are not. We refer to these as "death equivalents", i.e., the number of avoided deaths equal in value to the adaptation costs incurred. Note that the use of the these units is why adaptation costs in expression (iv) are multiplied by $\frac{1}{VSL}$, as the definition of adaptation costs $A(\cdot)$ in Equation 6 is given in dollars.

The full mortality risk of climate change for 24,378 global regions. Figure 8 shows the spatial distribution of the full mortality risk of climate change (expression (iv)) in 2100 under the emissions scenario RCP8.5, expressed in death-equivalents per 100,000. All other measures of climate change impacts (expressions (i)–(iii)) are mapped in Appendix Figure F.1. To construct these estimates, we generate impact-region specific predictions of mortality damages from climate change for all years between 2015 and 2100 (equal to expression (iii)), separately for each age group. Following the approach outlined in Section 4.3, we simultaneously compute associated measures of adaptation costs for each location and age at each point in time, and add them to expression (iii). The map displays the spatial distribution of the climate-induced death equivalent (expression (iv)), depicting the mean estimate across our ensemble of Monte Carlo simulations, accounting for both climate and statistical uncertainty and pooling across all age groups.[45] The density plots for select cities show the full distribution of impacts across all Monte Carlo simulations, with the white line equal to the mean estimate displayed on the map.

Figure 8 makes clear that the costs of climate change induced mortality risks are distributed unevenly around the world. Despite the gains from adaptation shown in Figure 7, there are large

[45]When calculating mean values across estimates generated for each of the 33 climate models that form our ensemble, we use model-specific weights. These weights are constructed as described in Appendix B.2.3 in order to accurately reflect the full probability distribution of temperature responses to changes in greenhouse gas concentrations.

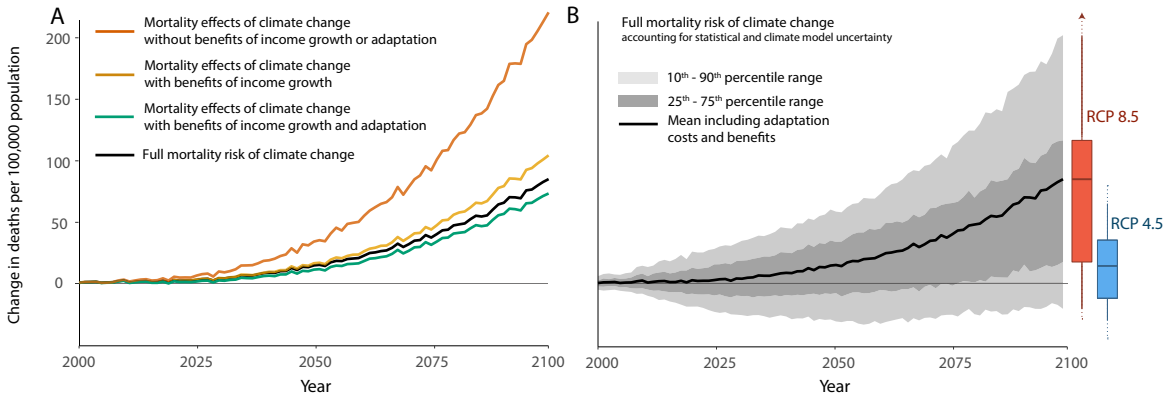

Figure 9: Time series of projected mortality risk of climate change. All lines show predicted mortality effects of climate change across all age categories and are represented by a mean estimate across a set of Monte Carlo simulations accounting for both climate model and statistical uncertainty. In panel A, each colored line represents a partial mortality effect, while the black line shows the full mortality risk due to climate change, accounting for both adaptation costs and benefits. Orange (expression (i)): mortality effects without adaptation. Yellow (expression (ii)): mortality effects with benefits of income growth. Green (expression (iii)): mortality effects with benefits of income growth and adaptation. Black (expression (iv)): full mortality risk calculated as the sum of mortality effects with adaptation and income growth benefits plus estimates of costs incurred to achieve adaptation, measured in units of death equivalents. Panel B shows the 10^{th}-90^{th} percentile range of the Monte Carlo simulations for the full mortality risk of climate change (black line in panel A), as well as the mean and interquartile range. The boxplots show the distribution of full mortality risk impacts in 2100 under both RCPs. All line estimates shown refer to the RCP8.5 emissions scenario and all line and boxplot estimates refer to the SSP3 socioeconomic scenario. Figure F.5 shows the equivalent for SSP3 and RCP4.5.

increases in mortality risk in the global south. For example, in Accra, Ghana, climate change is predicted to cause damages equivalent to approximately 160 additional deaths per 100,000 annually under RCP8.5 in 2100. In contrast, there are gains in many impact regions in the global north, including in Oslo, Norway, where we predict that the equivalent of approximately 230 lives per 100,000 are saved annually. These changes are equal to an 18% increase in Accra's annual mortality rate and a 28% decline in Oslo's.

Aggregate global mortality consequences of climate change. Figure 9 plots predictions of global increases in the mortality rate (deaths per 100,000, including death equivalents for adaptation costs) for all four measures of climate change impacts, under emissions scenario RCP8.5. The measures are calculated for each of the 24,378 impact regions and then aggregated to the global level. In panel A, each line shows a mean estimate for the corresponding climate change impact measure and year. Averages are taken across the full set of Monte Carlo simulation results from all 33 climate models and all draws from the empirical distribution of estimated regression parameters, as described in Section 4.6. In panel B, the 25^{th}-75^{th} and 10^{th}-90^{th} percentile ranges of the Monte Carlo simulation distribution are shown for the full mortality risk of climate change (expression (iv)); the black line represents the same average value in both panels. Boxplots to the right summarize the distribution of mortality impacts for both RCP8.5 and the moderate emissions scenario of RCP4.5, and Figure F.5 replicates the entire figure for RCP4.5.

Figure 9A illustrates that the mortality cost of climate change would be 221 deaths per 100,000 by 2100, on average across simulation runs (orange line), if the beneficial impacts of adaptation and income are shut down. This is an enormously large estimate; if it were correct, the mortality costs of climate change would be roughly equivalent in magnitude to all global deaths from cardiovascular disease

today (WHO, 2018). However, we estimate that future income growth and adaptation to climate substantially reduce these impacts. Higher incomes lower the mortality effect of climate change to an average of 104 deaths per 100,000 in 2100 (yellow line); climate adaptation reduces this further to 73 deaths per 100,000 (green line). Although substantially lower than the *no adaptation* projection, these smaller counts of direct mortality remain economically meaningful—for comparison, the 2017 mortality rate from automobile accidents in the United States was 11.4 per 100,000.

Figure 9A also demonstrates that climate adaptation is projected to be costly. Our estimates of climate adaptation costs are valued at 12 death-equivalents per 100,000 in 2100. The net result is that the full mortality risk due to climate change (i.e., expression (iv)) is projected to equal to 85 deaths per 100,000 by the end of the century under RCP8.5. Had we accounted for the benefits of adaptation but failed to account for their costs, we would have underestimated the total aggregate impact of these changes, particularly in regions of the world where adaptation costs compose a substantial share of total damages.[46] Nonetheless, our estimate for the global average benefits of adaptation (31 deaths per 100,000) outweighs the costs of these adjustments (12 death-equivalents per 100,000), demonstrating that the adaptation surplus discussed in Section 2 and detailed in Appendix A.2 is substantial.

The values in Figure 9A are mean values aggregated across results from 33 high-resolution climate models and all Monte Carlo simulation runs. However, the full distribution of our estimated damages across climate models (panel B of Figure 9) is right-skewed with a tail of potential mortality risk far higher than our central estimate. As evidence of this, the *median* value of the full mortality risk of climate change under RCP8.5 at end of century is 56 deaths per 100,000, as compared to a *mean* value of 85 and a 10^{th} to 90^{th} percentile range of [-21, 202].

Figure 9B and Appendix Figure F.3 show the expected implications of emissions mitigation. The average estimate of the full mortality risk of climate change of 85 deaths per 100,000 by the end of the century under RCP8.5 falls to 14 under the emissions stabilization scenario of RCP4.5 (where emissions decline after 2050). For RCP4.5, the median end-of-century estimate is 9, and the 10^{th} to 90^{th} percentile range is [-30, 65]. As a point of comparison to the prior literature, we compare these results to the FUND model, which is unique among the IAMs for calculating separate mortality impacts as a component of its SCC calculation. Although it is difficult to make a direct comparison due to differences in scenarios and lack of adaptation costs in the FUND estimates, the closest analog is to compare our estimates including adaptation benefits but not adaptation costs, a change of 73 deaths per 100,000 by 2100, to FUND's change of -2 deaths per 100,000 in the same year (Tol, 1997).[47]

A limit of our empirical approach is that we must sometimes extrapolate response functions to temperatures outside of those historically observed within our data. To address the concern that out-of-sample behavior is disproportionately influencing our results, we repeat the projections of mortality risk changes with two extra sets of restrictions imposed upon our empirically-estimated response functions. These two restrictions, described in Appendix F.3, involve either forcing the response function to be flat for all temperatures outside the observed range, *or* setting the marginal effect to be linearly increasing in the out-of-sample regions with a slope equal to the slope at the edge of the observed range. Figure

[46] We previously noted considerable heterogeneity across age-groups in our results. We will take this into account in our approach to valuing mortality damages monetarily in subsequent sections, and we display the underlying age group heterogeneity of these projections in Appendix F.

[47] This value was calculated by running the FUND model and extracting quantities from each sector of the model separately.

F.9 reveals that these two restrictions on out-of-sample behavior have negligible effects on our overall impacts. The value of the mortality impact of climate change including benefits of income growth and adaptation is approximately 1 death per 100,000 smaller by 2100 under RCP 8.5 in the case of the flat out-of-sample restriction.

Unequal distribution of mortality risk from climate change. Whether the full mortality risk caused by climate change is realized through actual deaths (first term in expression (iv)), as opposed to costly compensatory investments (second term in expression (iv)), differs substantially across the globe. While some locations suffer large increases in mortality rates, others avoid excess mortality through expensive adaptation. Figures 10A-C demonstrate that present day income is strongly correlated with the composition of future damages. In panel A, the negative correlation indicates that today's poor locations tend to suffer large increases in mortality rates by end of century, while mortality rates tend to decline due to climate change in today's rich locations. However, there is large variance across impact regions within each income decile, implying that some poor regions are projected to experience mortality rate declines, and some wealthy regions mortality rate increases. In panel B, the positive correlation indicates that wealthier locations are predicted to pay for future adaptive investments, while such costs are predicted to be much smaller in poor parts of the globe. Panel C shows that the full mortality risk of climate change, the sum of both deaths and adaptation costs measured in death-equivalents, is still borne disproportionately by regions that are poor today. On average, we find that in the poorest decile of today's income distribution, just 9% of the total burden of climate change induced mortality risk is borne as adaptation costs. In contrast, in the richest decile, on average approximately 3 lives are saved per 100,000 in 2100 due to climate change, while adaptation costs are three times larger than they are in today's poorest regions. It is also apparent that poorer regions face higher uncertainty in the magnitude of their projected impacts (Figure F.6). Similar figures in panels D–F demonstrate that the hottest locations today suffer the largest increase in death rates, while the coldest pay the highest adaptation costs. The impacts in the top decile of the current long-run climate distribution are noteworthy and raise questions about the habitability of these locations at the end of the century.

Climate change projection scenarios. The results in this section illustrate a single benchmark emissions and socioeconomic scenario (RCP8.5, SSP3). In Appendix F we report on the sensitivity of the results to alternative choices about the economic and population scenario, the emissions scenario, and assumptions regarding the rate of adaptation. These exercises underscore that the projected impacts of climate change over the remainder of the 21^{st} century will depend greatly on difficult-to-predict factors such as policy, technology, and demographics. However, we note that under both emissions scenarios RCP8.5 and RPC4.5, under all SSP scenarios, and under an alternative projection in which the rate of adaptation is deterministically slowed, the average estimate of the full mortality risk due to climate change is positive (both RCPs) and steadily increasing (RCP8.5) throughout the 21^{st} century.

Monetized value of the full mortality risk of climate change To monetize the full mortality risk of climate change, we use the value of a statistical life (VSL) to convert changes in mortality rates into dollars. Our primary approach relies on the U.S. EPA's VSL estimate of $10.95 million

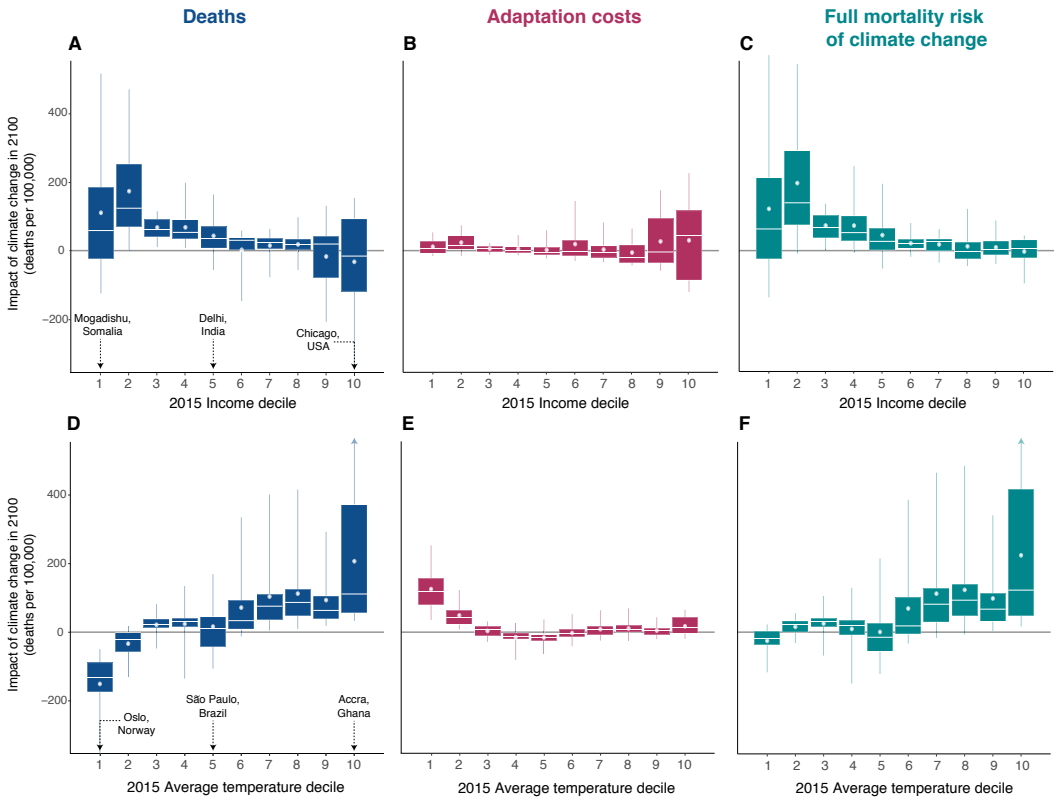

Figure 10: Climate change impacts and adaptation costs are correlated with present-day income and climate. Panels A and D show the change in annual mortality rates due to climate change in 2100 (RCP8.5, SSP3), accounting for the benefits of adaptation and income growth, against deciles of 2015 per capita income (A) and average annual temperature (D). Panels B and E show the annual adaptation costs incurred due to climate change in 2100, measured in death equivalents, from the same regions. Panels C and F show the full mortality risk due to climate change, which is the sum of deaths and adaptation costs measured in death equivalents. The income and average temperature deciles are calculated across 24,378 global impact regions and are population weighted using 2015 population values. All box plots show statistics of the distribution of estimated mean impacts across impact regions within a decile, where means are taken for each impact region across Monte Carlo simulations that account both for econometric and climate model uncertainty. Solid vertical lines in each box plot extend to the 5^{th} and 95^{th} percentiles of this distribution, boxes indicate the interquartile range, white horizontal lines indicate the median, and white circles indicate the mean.

(2019 USD).[48] We transform the VSL into a value per life-year lost using a method described in Appendix H.1, which allows us to compute the total value of expected life-years lost due to climate change, accounting for the different mortality- temperature relationships among the three age groups documented above. We allow the VSL to vary with income, as the level of consumption affects the relative marginal utilities of a small increment of consumption and a small reduction in the probability of death. Consistent with existing literature (e.g., Viscusi, 2015), in our primary estimate we use an income elasticity of unity to adjust the U.S. estimates of the VSL to different income levels across the

[48]This VSL is from the 2012 U.S. EPA Regulatory Impact Analysis (RIA) for the Clean Power Plan Final Rule, which provides a 2020 income-adjusted VSL in 2011 USD, which we convert to 2019 USD. This VSL is also consistent with income- and inflation-adjusted versions of the VSL used in the U.S. EPA RIAs for the National Ambient Air Quality Standards (NAAQS) for Particulate Matter (2012) and the Repeal of the Clean Power Plan (2019), among many other RIAs.

world and over time.[49] When computing the mortality partial SCC in Section 6, we provide multiple alternative valuation scenarios in addition to this benchmark case.

Using the SSP3 socioeconomic scenario, we find that under RCP8.5, our benchmark monetized value of the full mortality risk of climate change in 2100 amounts to 3.2% of global GDP on average, with an interquartile range of [-5.4%, 9.1%]. In contrast, under RCP4.5, this value falls to just 0.6% [-3.9%, 4.6%] of global GDP in 2100. While a direct comparison to leading IAMs is made difficult by the use of distinct socioeconomic scenarios and climate models, among many other factors, these mortality-related damages amount to ∼49-135% of the damages reported for *all sectors of the economy* in FUND, PAGE, and DICE, when the damage functions from each model are evaluated at the mean end-of-century warming observed in our multi-model ensemble under RCP8.5. Under RCP4.5, our mortality-related damages amount to 32-61% of the damages from DICE and PAGE, while damages from FUND are negative at RCP4.5 levels of warming.[50] It is apparent that this paper's results indicate that the mortality risks from climate change are much greater than had previously been understood. Some plausible scenarios suggest that, by themselves, they are larger than previous understanding of climate change's *full* impacts in 2100. The uncertainty around these estimates is also meaningful and while we leave explicit pricing of this uncertainty to future work, accounting for it would only increase the estimated welfare loss.

6 Results II: Partial mortality social cost of carbon

Section 5.3 provided results for the first key goal of this analysis: empirical estimates of the full mortality risk of climate change at high resolution across the globe, for individual years and two emissions scenarios. Here, we take on the second goal of the analysis: to monetize the full mortality-related social cost generated by the emission of a marginal ton of CO_2 (defined in Equation 9). This calculation represents the component of the *total* SCC that is mediated through excess mortality, but it leaves out adverse impacts in other sectors of the economy, such as reduced labor productivity or changing food prices. Hence, it is a mortality *partial* SCC.

One of two key building blocks of this exercise is an empirically-derived "damage function" (Nordhaus, 1992; Hsiang et al., 2017), which describes economic losses to an economy as a function of the change in the global climate. It is necessary to develop time-varying damage functions in our context, because the mortality sensitivity of temperature and total monetized impacts of climate change evolve over time due to changes in per capita income and the underlying population. Thus, the damages from a marginal change in emissions will vary depending on the year in which they are evaluated. Importantly, these damage functions are fully differentiable, so when they are combined with climate model output determining the change in warming arising from any emissions trajectory, it is possible to determine the losses from a marginal increase in emissions. The second key building block is a

[49]The EPA considers a range of income elasticity values for the VSL, from 0.1 to 1.7 (U.S. Environmental Protection Agency, 2016b), although their central recommendations are 0.7 and 1.1 (U.S. Environmental Protection Agency, 2016). A review by Viscusi (2015) estimates an income-elasticity of the VSL of 1.1.

[50]To conduct this comparison, we use the damage functions reported for each IAM in the Interagency Working Group on Social Cost of Carbon (2010), which are indexed against warming relative to the pre-industrial climate. We evaluate each damage function at the mean end-of-century warming (4°C for RCP8.5 and 1.8°C for RCP4.5) across the SMME climate model ensemble used in our analysis, after adjusting warming to align pre-industrial temperature anomalies from the IAMs with the anomalies relative to 2001-2010 from our analysis (Lenssen et al., 2019).

climate model that is capable of simulating climate trajectories far into the future, and can capture the global climate response of a marginal emission today. Combined, these two elements characterize a trajectory of global impacts, which can then be valued and discounted to inform decisions today.

In this section, we transform monetized projections of deaths due to climate change from Section 5.3 into damage functions for excess mortality risk. We then use these time-varying empirical damage functions to compute marginal costs from a marginal CO_2 emission, which is the mortality partial SCC.

6.1 Constructing damage functions for excess mortality risk

For this paper, damage functions describe the total monetized losses due to changes in mortality risk, inclusive of adaptation benefits and costs, as a function of the change in *global mean surface temperature* (ΔGMST), our empirical estimate of the change in the global climate.[51] Due to differences in the character of climate projections pre- and post-2100, and lack of available socioeconomic projections after 2100, this subsection details some important differences in the approach for calculation of damage functions before and after 2100. Additionally, it explains the approach to account for damage function uncertainty.

Computing damage functions through 2100. We estimate a set of time-varying quadratic damage functions that relate the total global value of mortality-related climate change damages (D) to the magnitude of global warming (ΔGMST):

$$D(\Delta GMST, t)_{irmt} = \alpha^t + \psi_1^t \Delta GMST_{rmt} + \psi_2^t \Delta GMST_{rmt}^2 + \varepsilon_{irmt} \tag{13}$$

To construct the data necessary to estimate Equation 13, damages (D_{irmt}) are computed in each year (t) using many climate models (m), two emissions scenarios (r), and a resampling of the econometric parameters recovered from estimation of the mortality-temperature relationship in Equation 6 (i). These multiple simulations lead to an empirically-derived distribution of potential economic outcomes that are conditional on the ΔGMST value determined by each climate model in each year for each emissions scenario.[52] To estimate Equation 13 for year t, we fit a quadratic function through these simulated outcomes, using all 9,750 Monte Carlo simulation runs within a 5-year window of t, thereby allowing $D(\Delta GMST, t)_{irmt}$ to evolve flexibly over the century. We note that pre-2100 damage functions are indistinguishable if we use a third-, fourth- or fifth-order polynomial, and we show robustness of our mortality partial SCC estimates to functional form choice in Appendix H.4.

Figure 11A illustrates the procedure for $t = 2097$, with D_{irmt} estimates from all Monte Carlo simulations shown as points[53] located along the horizontal axis based on their corresponding ΔGMST_{irmt}.

[51] *Global mean surface temperature* is defined as the global area-weighted average of surface air temperature over land and sea surface temperature over the oceans. Our climate change impacts are calculated relative to a baseline of 2001-2010. Therefore, we define changes in global mean surface temperature (ΔGMST) as relative to this same period.

[52] Note that the ΔGMST value in each climate model is a summary parameter, resulting from the complex interaction of many physical elements of the model, including the *equilibrium climate sensitivity*, a number that describes how much warming is associated with a specified change in greenhouse gas emissions. Differences in the spatial distributions of warming across models, and their mapping on populations around the world, remain an additional unresolved uncertain element of climate models that are idiosyncratic to each model.

[53] This scatterplot includes realizations under all RCP4.5 and RCP8.5 scenarios for all projections in our 33-member ensemble under our benchmark method of valuation – the age-invariant EPA VSL with an income elasticity of one applied to all impact regions – in the end-of-century years 2095-2100. See Appendix H for results across different

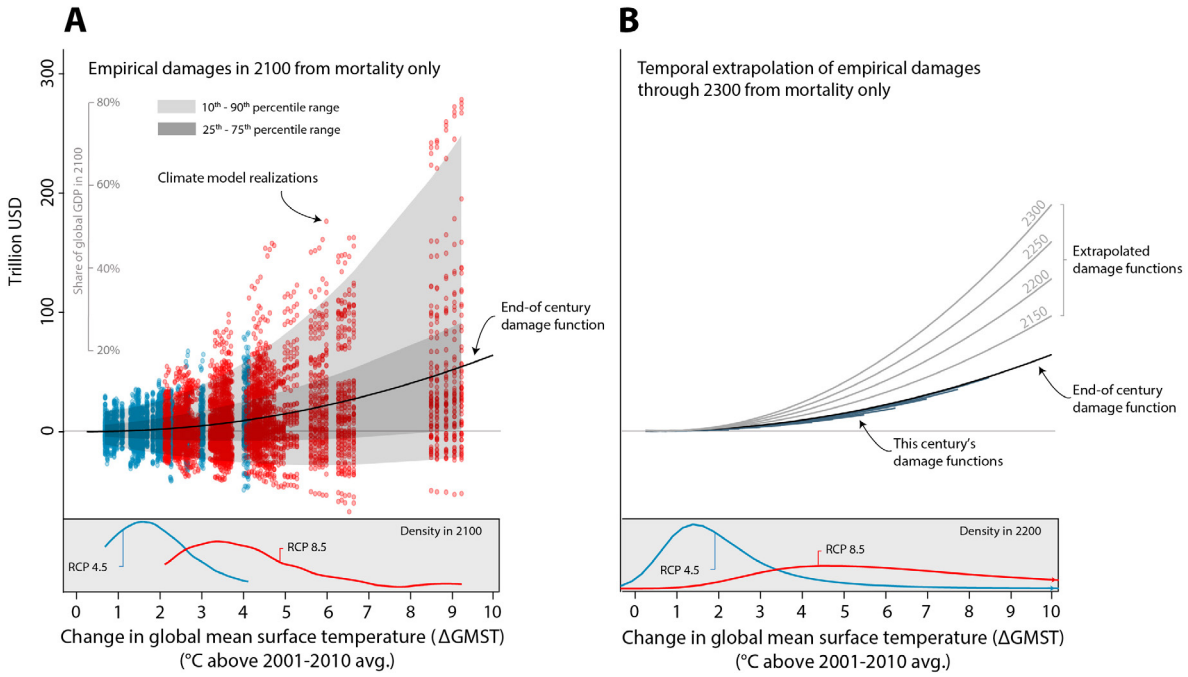

Figure 11: Empirically-derived mortality-only damage functions. Both panels show damage functions relating empirically-derived total global mortality damages to anomalies in global mean surface temperature (ΔGMST). In panel A, each point (red = RCP8.5, blue = RCP4.5) indicates the value of the full mortality risk of climate change in a single year (ranging from 2095 to 2100) for a single simulation of a single climate model, accounting for both costs and benefits of adaptation. The black line is the quadratic damage function estimated through these points. The distribution of temperature anomalies at end of century (2095-2100) under two emissions scenarios across our 33 climate models is in the bottom panel. In panel B, the end-of-century damage function is repeated. Damage functions are shown in dark blue for every 10 years pre-2100, each of which is estimated analogously to the end-of-century damage function and is shown covering the support of ΔGMST values observed in the SMME climate models for the associated year. Damage functions are shown in light grey for every 50 years post-2100, each of which is extrapolated. Our projection results generate mortality damages only through 2100, due to limited availability of climate and socioeconomic projections for years beyond that date. To capture impacts after 2100, we extrapolate observed changes in damages over the 21^{st} century to generate time-varying damage functions through 2300. The distribution of temperature anomalies around 2200 (2181-2200) under two emissions scenarios using the FAIR simple climate model is in the bottom panel. To value lives lost or saved, in both panels we use the age-varying U.S. EPA VSL and an income elasticity of one applied to all impact regions.

The median end-of-century warming relative to 2001-2010 under RCP8.5 (red points) across our climate models is +3.7°C, while under RCP4.5 (blue points) it is +1.6°C. The black line is the quadratic damage function estimated for the year 2097, the latest year for which a full 5-year window of damage estimates can be constructed. The estimated damage function in 2097 recovers total (undiscounted) damages with an age-varying VSL at 3.7°C and 1.6°C of $7.8 and $1.2 trillion USD, respectively. Analogous curves are constructed for all years, 2015 to 2100.

Computing post-2100 damage functions. Even with standard discount rates, a meaningful fraction of the present discounted value of damages from the release of CO_2 today will occur after 2100 (Kopp and Mignone, 2012), so it is important to develop post-2100 damage functions. The pre-2100 approach cannot be used for these later years because only 6 of the 21 GCMs that we use to build our SMME ensemble (see Section 3.2) simulate the climate after 2100 for both RCP scenarios. Similarly,

valuation assumptions. Due to the dependence of damages D on GDP per capita and on demographics, we estimate separate damage functions for every SSP scenario. Results across different scenarios are shown in Appendix H.

the SSPs needed to project the benefits of income growth and changes in demographic compositions also end in 2100.

To estimate post 2100-damages, we develop a method to extrapolate changes in the damage function beyond 2100 using the observed evolution of damages near the end of the 21^{st} century. The motivating principle of our extrapolation approach is that these observed changes in the shape of the damage function near the end of the century provide plausible estimates of future damage function evolution after 2100. This reduced-form approach allows our empirical results to constrain and guide a projection to years beyond 2100. To execute this extrapolation, we pool values D_{irmt} from 2085-2100 and estimate a quadratic model similar to Equation 13, but interacting each term linearly with year t.[54] This allows estimation of a damage surface as a parametric function of year, which can then be used to predict extrapolated damage functions for all years after 2100, smoothly transitioning from our climate model-based damage functions prior to 2100. Appendix G provides a detailed explanation of the approach.

The approach produces post-2100 damage functions that become more convex over time, suggesting larger damages for a given level of warming. This finding comes directly from the estimation of Equation 13 that found that in the latter half of the 21^{st} century the full mortality damages are larger when they occur later, holding constant the degree of warming. This finding that mortality costs rise over time is the net result of countervailing forces. On the one hand, damages are larger in later years because there are larger and older populations[55] with higher VSLs due to rising incomes. On the other hand, damages are smaller in later years because populations are better adapted due to higher incomes and a slower rate of warming projected in later years. Our results suggest the former dominates by end of century, causing damages to be trending upward when high-resolution simulations end in 2100.

Panel B of Figure 11 illustrates damages functions every 10 years prior to 2100, as well as extrapolated damage functions for the years 2150, 2200, 2250, and 2300. In dollar terms, these extrapolated damages continue to rise post-2100 and become steeper, as they did pre-2100. In Appendix H, we explore the importance of this extrapolation by using an alternative approach to estimating post-2100 damages, instead calculating partial SCC estimates using a damage function frozen at its 2100 shape for all years 2101-2300. With this alternative approach, our central estimate of the mortality partial SCC falls 21%, indicating that extrapolation of the damage function has a modest impact on our partial SCC estimates, due in part to the important role of discounting (Table H.6).

Accounting for uncertainty in damage function estimation. As discussed, there is substantial uncertainty in projected mortality effects of climate change due to statistical uncertainty in the estimation of mortality-temperature response functions. The approach described above details the estimation of a damage function using the conditional expectation function through the full distribution of simulation results. In addition to reporting the predicted damages resulting from this damage function describing (conditional) expected values, we also estimate a set of quantile regressions to capture the full distribution of simulated mortality impacts.[56] Just as above for the mean damage function, extrapolation past the year 2100 is accomplished using a linear time interaction, estimated separately for each quantile. Central estimates of the mortality partial SCC reported below use the mean regression,

[54] We use 2085-2100 because the evolution of damages over time becomes roughly linear conditional on ΔGMST by this period.

[55] In SSP3, the share of the global population in the most vulnerable >64 age category rises from 8.2% in 2015 to 16.2% in 2100.

[56] We estimate a damage function for every 5^{th} percentile from the 5^{th} to 95^{th}.

while ranges incorporating damage uncertainty use the full set of time-varying quantile regressions.

6.2 Computing marginal damages from a marginal carbon dioxide emissions pulse

We empirically approximate the mortality partial SCC for emissions that occur in the year 2020 (Equation 9) as:

$$\textit{Mortality partial } SCC_{2020} \approx \sum_{t=2020}^{2300} e^{-\delta(t-2020)} \frac{\partial \hat{D}(\Delta GMST, t)}{\partial \Delta GMST_t} \frac{d\Delta GMST_t}{dCO2_{2020}}, \tag{14}$$

where ΔGMST approximates the multi-dimensional climate vector $\boldsymbol{C}$, we use changes in CO_2 to represent changes in global emissions E,[57] we assume that discounted damages from an emissions pulse in year 2020 become negligible after 2300, and we approximate the integral in Equation 9 with a discrete sum using time steps of one year. The values $\frac{\partial \hat{D}(\Delta GMST,t)}{\partial \Delta GMST_t}$ are the marginal damages at each moment in time that occur as a result of this small change in all future global temperatures; they are computed using the damage functions described in the last subsection.

The term $\frac{d\Delta GMST_t}{dCO2_{2020}}$ is the increase in ΔGMST that occurs at each moment in time along a baseline climate trajectory as a result of a marginal unit of emissions in 2020, which we approximate with an "infinitesimally small" pulse of CO_2 emissions. Its estimation requires a climate model capable of estimating the global temperature response in each year to a single pulse of CO_2 emissions. Because we are interested in computing this value for a large number of scenarios, including ones that reflect scientific uncertainty about the physical magnitude and timing of warming, referred to as the *global climate sensitivity*, we use a "simple climate model" to estimate $\frac{d\Delta GMST_t}{dCO2_{2020}}$.

Applying a simple climate model to the damage function. To calculate the change in ΔGMST_t due to a marginal pulse of CO_2 in 2020, we use the Finite Amplitude Impulse Response (FAIR) simple climate model that has been developed especially for this type of calculation (Millar et al., 2017).[58] We use FAIR to calculate ΔGMST_t trajectories for emissions scenarios RCP4.5 and RCP8.5, both with and without an exogenous impulse of 1 gigaton C (equivalent to 3.66Gt CO_2) in the year 2020, an approximation of an infinitesimal emission for which the model numerics are stable. In FAIR, this emissions impulse perturbs the trajectory of atmospheric CO_2 concentrations and ΔGMST for 2020-2300, with dynamics that are influenced by the baseline RCP scenario. In each scenario, the trajectory of ΔGMST_t in the "RCP + pulse" simulation is differenced from the baseline "RCP only" simulation to compute $\frac{d\Delta GMST_t}{dCO2_t}$, and the resulting damages are converted into USD per one ton CO_2. There is naturally uncertainty in these trajectories, and our approach accounts for uncertainty associated with four key parameters of the FAIR model (i.e., the transient climate response, equilibrium climate sensitivity, the short thermal adjustment time, and the time scale of rapid carbon uptake by the ocean mixed layer). This approach, detailed in Section G, ensures that the distribution of transient warming responses we use to generate partial SCC values matches the

[57] We use CO_2 to represent changes in all global greenhouse gas (GHG) emissions as it is the most abundant GHG and the warming potential of all other GHGs are generally reported in terms of their CO_2 equivalence.

[58] FAIR is a zero-dimensional structural representation of the global climate designed to capture the temporal dynamics and equilibrium response of ΔGMST to greenhouse gas forcing. Appendix G shows that our simulation runs with FAIR create ΔGMST distributions that match those from the climate projections in the high-resolution models in the SMME.

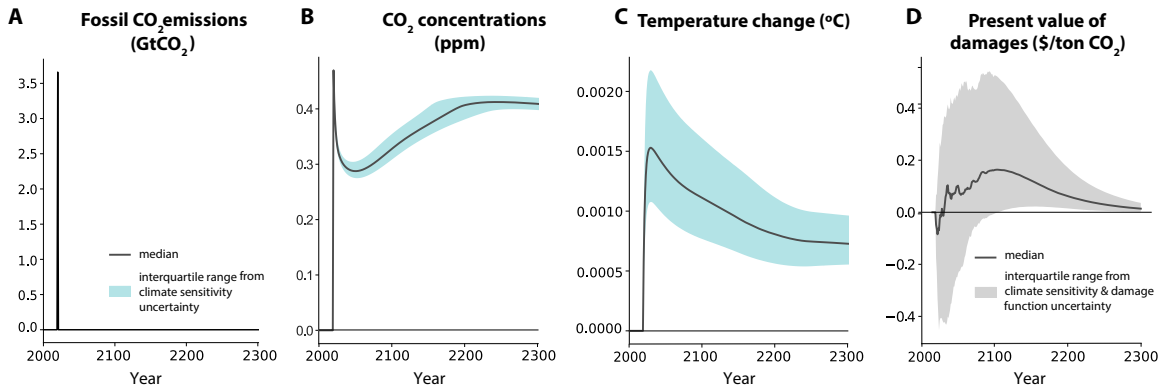

Figure 12: Change in emissions, concentrations, temperature, and damages due to a marginal emissions pulse in 2020. Panel A shows a 1GtC emissions pulse (equivalent to 3.66Gt CO_2) in 2020 for emissions scenario RCP8.5. Panel B displays the effect of this pulse on atmospheric CO_2 concentrations, relative to the baseline. In panel C, the impact of the pulse of CO_2 on temperature is shown where the levels are anomalies in global mean surface temperature (GMST) in Celsius. In panels A-C, shaded areas indicate the inter-quartile range due to climate sensitivity uncertainty, while solid lines are median estimates. Panel D shows the change in discounted damages over time due to a 1 Gt pulse of CO_2 in 2020, as estimated by our empirically-derived damage functions, using a 2% annual discount rate and the age-varying EPA VSL. The shaded area indicates the inter-quartile range due to climate sensitivity and damage function uncertainty, while the solid line is the median estimate.

corresponding distributions from the IPCC Assessment Report 5 (AR5).

Summarizing the impacts of a marginal increase in CO_2 emissions Figure 12 graphically depicts the difference between the "RCP + pulse" and baseline RCP trajectories for four key outcomes.[59] The pulse in emissions is shown in panel A. Its influence on CO_2 concentrations is reported in panel B; the immediate decline followed by a century-long increase is largely due to dynamics involving the ocean's storage and release of emissions. Panel C displays the resulting change in temperature, which makes clear that a pulse today will influence temperatures for over three centuries. The shaded green area in panels A-C represents the inter-quartile range of each year's outcome, and reflects uncertainty in the climate system (see Appendix G for details).

Panel D plots the discounted (2% discount rate) stream of damages due to this marginal pulse of emissions. The temporal pattern of the present value of mortality damages reflects the nonlinearity of the damage function (e.g., Figure 11), which itself depends on nonlinearities in location-specific mortality-temperature relationships (e.g., Figure 5), as well as the discount rate and the dynamic temperature response to emissions (panel C). The peak damages from a ton of CO_2 emissions are \$0.16 in year 2104; by year 2277, annual damages are always less than \$0.02. It is noteworthy that 67.9% of the present value of damages occur after the year 2100. The shaded grey area represents the inter-quartile range of each year's outcome, and reflects uncertainty in the climate system as well as uncertainty in the damage function. RCP 4.5 results are shown in Figure G.3 and additional details are in Appendix G.

[59] Using the trajectories in Figure 12 is consistent with the "SCC experiment" that is used in IAMs to calculate an SCC (National Academies of Sciences, Engineering, and Medicine, 2017). We discuss uncertainties in FAIR configuration parameters below and in Appendix G. The median values of parameter-specific distributions used for the central mortality partial SCC estimate include a transient climate response (TCR) of 1.6 and an equilibrium climate sensitivity (ECS) of 2.7.

6.3 Estimates of the partial social cost of carbon due to excess mortality risk

Table 3 reports mortality partial SCC estimates. The columns apply four different annual discount rates – three used in prior estimates of the SCC (2.5%, 3%, and 5%) (Interagency Working Group on Social Cost of Carbon, 2010; National Academies of Sciences, Engineering, and Medicine, 2017), and one lower rate that aligns more closely with recent global capital markets (2%) (Board of Governors of the US Federal Reserve System, 2020). Panel A uses the U.S. EPA's VSL of $10.95 million (2019 USD), transformed into value per life-year lost (see Appendix H.1 for details). This accounts for the different mortality-temperature relationships among the three age groups documented above.[60] Panel B uses age-invariant values of the VSL. Both valuations adjust for cross sectional variation in incomes among contemporaries and global income growth. Appendix H presents results under a wide range of additional valuation scenarios, including an alternative and lower Ashenfelter and Greenstone (2004) VSL of $2.39 million (2019 USD),[61] and an approach where the VSL is adjusted only based on global average income such that the lives of contemporaries are valued equally, regardless of their relative incomes.

The estimates in Table 3 utilize the median values of FAIR's four key parameter distributions and the mean global damage function. Interquartile ranges (IQRs) are reported, reflecting uncertainty in climate sensitivity (uncertainty in the simple climate model FAIR) and in the damage function (which includes uncertainty arising from econometric estimation and from climate model uncertainty regarding the spatial distribution of warming). All values represent the global sum of each impact region's MWTP today (2019 USD) to avoid the release of an additional metric ton of CO_2 in 2020, including both the costs and benefits of adaptation.

In column 1 and panel A of Table 3, we report partial SCC values under a $\delta = 2\%$ discount rate and using an age-varying VSL. Under this valuation approach, the mortality partial SCC is $17.1 [-$24.7, $53.6] for the low to moderate emissions scenario and $36.6 [-$7.8, $73.0] for the high emissions scenario. We highlight a 2% discount rate because it conservatively reflects changes in global capital markets over the last several decades: while the Interagency Working Group on Social Cost of Greenhouse Gases (2016) recommends a discount rate of 3%, the average 10-year Treasury Inflation-Indexed Security value over the available record of this index (2003-present) is just 1.01% (Board of Governors of the US Federal Reserve System, 2020). We show results for a discount rate of 1.5% in Appendix Table H.5. We emphasize the age-varying VSL approach because standard economic reasoning implies that valuation of life lost should vary by age (Jones and Klenow, 2016; Murphy and Topel, 2006).

When following the Interagency Working Group on Social Cost of Greenhouse Gases (2016) preference for a discount rate of $\delta = 3\%$ and the use of an age-invariant VSL, the central estimate of the mortality partial SCC is $6.7 per metric ton of CO_2 for the low to moderate emissions scenario (RCP4.5), with an IQR of [-$15.7, $32.1], and $22.1 [-$5.6, $53.4] per metric ton for the high emissions scenario (RCP8.5).

[60] In the main text, a simple life-years calculation that assigns each life-year lost the same economic value is used. In Appendix H, we also show calculations that adjust the value of remaining life by age at death using the estimates of age-specific value of remaining life from Murphy and Topel (2006), which produces results that differ only slightly from those under the primary approach.

[61] See Appendix Table H.1 for a comparison of these VSL values with values from the OECD, which are higher than Ashenfelter and Greenstone (2004), but lower than the U.S. EPA's VSL.

Table 3: Estimates of a partial social cost of carbon for excess mortality risk incorporating the costs and benefits of adaptation

	Annual discount rate			
	$\delta = 2\%$	$\delta = 2.5\%$	$\delta = 3\%$	$\delta = 5\%$
Panel A: Age-adjusted globally varying value of a statistical life (2019 US Dollars)				
Moderate emissions scenario (RCP4.5)	17.1	11.2	7.9	2.9
Full uncertainty IQR	[-24.7, 53.6]	[-18.9, 36.0]	[-15.2, 26.3]	[-8.5, 11.5]
High emissions scenario (RCP8.5)	36.6	22.0	14.2	3.7
Full uncertainty IQR	[-7.8, 73.0]	[-10.6, 46.8]	[-11.4, 32.9]	[-8.9, 13.0]
Panel B: Globally varying value of a statistical life (2019 US Dollars)				
Moderate emissions scenario (RCP4.5)	14.9	9.8	6.7	1.7
Full uncertainty IQR	[-21.2, 63.5]	[-17.9, 43.5]	[-15.7, 32.1]	[-11.8, 14.7]
High emissions scenario (RCP8.5)	65.1	36.9	22.1	3.5
Full uncertainty IQR	[3.0, 139.0]	[-2.4, 83.1]	[-5.6, 53.4]	[-9.3, 16.0]

In both panels, an income elasticity of one is used to scale the U.S. EPA VSL value (alternative values using the VSL estimate from (Ashenfelter and Greenstone, 2004) are shown in Appendix H). All regions thus have heterogeneous valuation, based on local income. All SCC values are for the year 2020, measured in PPP-adjusted 2019 USD, and are calculated from damage functions estimated from projected results under the socioeconomic scenario SSP3 (alternative values using other SSP scenarios are shown in Appendix sec:appsccrobustness). In panel A, SCC estimates use an age adjustment that values deaths by the expected number of life-years lost, using an equal value per life-year (see Appendix H.1 for details and Appendix H.2 for alternative calculations that allow the value of a life-year to vary with age, based on Murphy and Topel (2006)). In panel B, SCC calculations use value of a statistical life estimates that do not vary with age. Point estimates rely on the median values of the four key input parameters into the climate model FAIR and a conditional mean estimate of the damage function. The uncertainty ranges are interquartile ranges [IQRs] including both climate sensitivity uncertainty and damage function uncertainty (see Appendix G for details).

Some other features of these results are worth underscoring. First, mortality partial SCC estimates for RCP4.5 are systematically lower than RCP8.5 primarily because the damage function is convex, so marginal damages increase in the high emissions scenario. Second, the combination of this convexity, which itself is accentuated at higher quantiles of the damage function, and the skewness of the climate sensitivity distribution causes the distribution of partial SCCs to also be right skewed with a long right tail. For example, the 95^{th} and 99^{th} percentiles of the partial SCC for $\delta = 2\%$ and an age-varying VSL for RCP8.5 are \$290.3 and \$704.1, respectively; with $\delta = 3\%$ and an age-invariant VSL these values are \$175.3 and \$391.9. Third, in Appendix G we show that uncertainty in the partial SCC is consistently dominated by uncertainty in the damage function, as opposed to uncertainty in climate sensitivity. Finally, while Table 3 reflects what we believe to be mainstream valuation and socioeconomic scenarios, Appendix Tables H.2-H.7 report estimates based on multiple alternative approaches. Naturally, the resulting SCC estimates vary under different valuation assumptions and baseline socioeconomic trajectories, and we point readers to these specifications for a more comprehensive set of results.

7 Limitations

As the paper has detailed, the mortality risk changes from climate change and the mortality risk partial SCC have many ingredients. We have tried to probe the robustness of the results to each of them, but there are four issues that merit special attention when interpreting the results, because they are outside the scope of the analysis.

Migration responses First, the estimates in the paper do not reflect the possibility of migration responses to climate change. If migration were costless, it seems likely that the mortality risk partial SCC would be smaller, as people from regions with high damages (such as sub-Saharan Africa) may move to regions with low or even negative damages (such as Scandinavia). However, both distant and recent history in the U.S. and around the globe underscores that borders are meaningful and that there are substantial costs to migration which might limit the scale of feasible migrations. Indeed, existing empirical evidence of climate-induced migration, based on observable changes in climate to date, is mixed (Carleton and Hsiang, 2016).

Humidity Second, our estimates do not directly incorporate the role of humidity in historical mortality-temperature relationships nor in projections of future impacts. There is growing evidence that humidity influences human health through making it more difficult for the human body to cool itself during hot conditions (e.g., Sherwood and Huber, 2010; Barreca, 2012). While temperature and humidity are highly correlated over time, they are differentially correlated across space, implying that our measures of heterogeneous mortality-temperature relationships may be influenced by the role of humidity. To date, lack of high-resolution historical humidity data and highly uncertain projections of humidity under climate change (Sherwood and Fu, 2014) have limited our ability to include this heterogeneity in our work. However, emerging work on this topic (Yuan, Stein, and Kopp, 2019; Li, Yuan, and Kopp, 2020) will provide opportunities to explore humidity in future research.

Technological change Third, the paper's projections incorporate advancements in technology that enhance adaptive ability, even though we have not explicitly modeled technological change. In particular, we allow mortality-temperature response functions to evolve in accordance with rising incomes and temperatures and do not restrict them to stay within the bounds of the current observed distribution of temperature responses. However, while our estimates reflect technical advancement as it historically relates to incomes and climate, they do not reflect the likely passing of climate-biased technical change that lowers the *relative* costs of goods which reduce the health risks of high temperatures. Therefore, the paper's results will overstate the mortality risk of climate change if directed technological innovations lower the relative costs of adapting to high temperatures.

Uncertainty Throughout this paper, we have emphasized central estimates of the mortality risk damages of climate change and the partial SCC, but also noted the meaningful uncertainty associated with these estimates. However, this paper's estimates of damages do not reflect efforts to price this uncertainty. With risk averse agents, this uncertainty would undoubtedly increase the estimates of the climate change mortality risk damages and the mortality partial SCC (Weitzman, 2011; Traeger, 2014).

8 Conclusion

This paper has outlined a new method for empirically estimating the costs of climate change for a single sector of the economy and implemented it in the context of mortality risks associated with temperature change. Specifically, we highlight two primary contributions: a framework for estimating the total impact of climate change on mortality risk both globally and for more than 24,000 regions that comprise the planet, and a framework for estimating a mortality partial SCC. There are several noteworthy methodological innovations and intermediate findings.

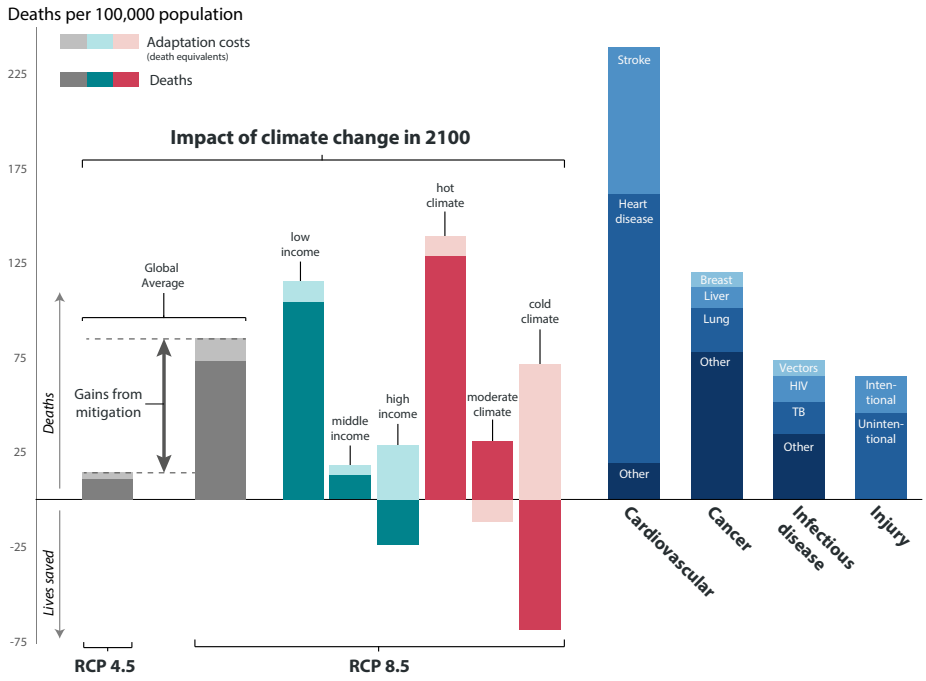

Figure 13: The impact of climate change in 2100 is comparable to contemporary leading causes of death. Impacts of climate change (grey, teal, and coral) are calculated for the year 2100 for SSP3 and include changes in death rates (solid colors) and changes in adaptation costs, measured in death equivalents (light shading). Global averages for RCP 8.5 and RCP 4.5 are shown in grey, demonstrating the gains from mitigation. Income and average climate groups under RCP8.5 are separated by tercile of the 2015 global distribution across all 24,378 impact regions. Blue bars on the right indicate average mortality rates globally in 2018, with values from WHO (2018). Figure F.7 provides an RCP4.5 version of this figure.

First, the relationship between mortality rates and temperature is highly nonlinear and varies with a location's income and climate. These findings were only possible due to the collection and analysis of highly resolved data covering roughly half of the world's population, which enabled us to estimate flexible empirical models relating mortality rates to temperature, climate, and income.

Second, the costs of climate change induced mortality risks are distributed unevenly across the 24,378 regions that we use to create local-level projections. For example, by 2100, we project that climate change will cause annual damages equivalent to approximately 160 additional deaths per 100,000 in Accra, Ghana, but will also generate annual benefits equivalent to approximately 230 lives per 100,000 in Oslo, Norway. To put these numbers in perspective, Figure 13 reveals that the projected

impact of climate change on mortality will be comparable globally to leading causes of death today, such as cancer and infectious disease. It also demonstrates the benefits from mitigation, as the end of century estimate of mortality risk of climate change falls from 85 deaths per 100,000 under RCP 8.5 to just 14 per 100,000 under RCP 4.5, though much of the inequality in impacts evidence here remains under RCP4.5 (see Figure F.7). Today's poor bear a disproportionately high share of the global mortality risks of climate change, as current incomes (as well as current average temperatures) are strongly correlated with future climate change impacts.

Third, the heterogeneous impacts appear to reflect investments that individuals and societies make based on the costs and benefits of responding to differences in climate. Estimated mortality impacts that do not account for adaptation overstate the mortality impacts of climate change in 2100 by more than a factor of 2.6. We outline and implement a revealed preference method to recover the costs of these adaptation investments, even though they cannot be directly observed. Notably, the degree to which the full mortality risk of climate change is realized through actual deaths, as opposed to costly adaptation, varies widely across space and time. For example, Figure 13 shows that today's poor locations tend to bear a larger share of the projected burden in the form of direct mortality impacts, while today's rich face large increases in projected adaptation costs.

Fourth, there is substantial climate and statistical uncertainty around these estimates and we find that the distribution of projected losses is right skewed; for example the mean loss in 2100 is about 51% larger than the median loss. Although we do not account for risk aversion, it is evident that doing so would increase the valuations of these impacts.

The paper's ultimate goal is to develop the first empirically grounded estimates of climate damages and partial SCC that reflects the consequences of climate change on mortality and investments in adaptation. The estimates suggest that the mortality risk damages account for 3.2% of global GDP in 2100 under a high emissions scenario and 0.6% under a moderate one. Our estimates of the mortality risk partial SCC imply that with a 2% discount rate and an age-varying VSL, the present value of excess mortality risk due to climate change imposed by a marginal metric ton of CO_2 emissions in 2020 is roughly \$36.6 [-\$7.8, \$73.0] (in 2019 USD) with a high emissions scenario (RCP8.5) and \$17.1 [-\$24.7, \$53.6] with a moderate one (RCP4.5), where brackets indicate interquartile ranges accounting for both climate sensitivity and damage function uncertainty. Under a 3% discount rate and age-invariant VSL, assumptions preferred by the Interagency Working Group on Social Cost of Carbon (2010), these values are \$22.1 [-\$5.6, \$53.4] and \$6.7 [-\$15.7, \$32.1], respectively.

These findings suggest that previous research has significantly understated climate change damages due to mortality. For example, the mortality damages we estimate in 2100 account for 49% to 135% of *total* damages across all sectors of the economy according to leading IAMs. Moreover, the mortality partial SCC reported here, under comparable valuation assumptions, is more than 10 times larger than the total health impacts embedded in the FUND IAM (Diaz, 2014).[62] Further, the high emissions and 3% discount rate partial SCC that is most similar to the scenario underlying the Obama Administration SCC produces an excess mortality partial SCC that is 44% of the Administration's *full* SCC.

The climate change challenge is considered existential by some and a relatively small risk by others,

[62]Diaz (2014) computes comparable partial SCC values for the FUND model (3% discount rate, "business as usual" emissions scenario) and reports values for three comparable health impacts (diarrhea, vector born diseases, and cardio-vascular/respiratory impacts) that total less than \$2.0 (2019 USD).

yet much of what is known about its overall impacts, particularly the SCC, comes from integrated assessment models that do not sit on a robust empirical foundation. In particular, many models currently used to compute the SCC are either not calibrated against data, have a calibration that is not documented, or are calibrated against empirical estimates that are not derived from modern empirical techniques and are unlikely to be globally representative. Advances in access to data and computing render these modeling choices unnecessary.

We believe that this paper has highlighted a key role for systematic empirical analysis in providing a clearer picture of how, why, and where costs of climate change are likely to emerge in the future. Looking ahead, this general approach developed in this paper can be applied to other aspects of the global economy besides mortality risk, and doing so is a promising area for future research.

References

Acemoglu, Daron, Simon Johnson, and James A. Robinson. 2001. "The Colonial Origins of Comparative Development: An Empirical Investigation." *American Economic Review* 91 (5):1369–1401. URL https://www.aeaweb.org/articles?id=10.1257/aer.91.5.1369.

Ashenfelter, Orley and Michael Greenstone. 2004. "Using mandated speed limits to measure the value of a statistical life." *Journal of Political Economy* 112 (S1):S226–S267.

Auffhammer, Maximilian. 2018a. "Climate adaptive response estimation: Short and long run impacts of climate change on residential electricity and natural gas consumption using big data." *NBER Working paper* .

———. 2018b. "Quantifying economic damages from climate change." *Journal of Economic Perspectives* 32 (4):33–52.

Auffhammer, Maximilian and Anin Aroonruengsawat. 2011. "Simulating the impacts of climate change, prices and population on California's residential electricity consumption." *Climatic Change* 109 (1):191–210. URL http://dx.doi.org/10.1007/s10584-011-0299-y.

Barreca, Alan, Karen Clay, Olivier Deschênes, Michael Greenstone, and Joseph S Shapiro. 2015. "Convergence in adaptation to climate change: Evidence from high temperatures and mortality, 1900–2004." *The American Economic Review* 105 (5):247–251.

Barreca, Alan, Karen Clay, Olivier Deschenes, Michael Greenstone, and Joseph S. Shapiro. 2016. "Adapting to climate change: The remarkable decline in the US temperature-mortality relationship over the twentieth century." *Journal of Political Economy* 124 (1):105–159. URL http://dx.doi.org/10.1086/684582.

Barreca, Alan I. 2012. "Climate change, humidity, and mortality in the United States." *Journal of Environmental Economics and Management* 63 (1):19–34.

Becker, Gary S. 2007. "Health as human capital: synthesis and extensions." *Oxford Economic Papers* 59 (3):379–410.

Board of Governors of the US Federal Reserve System. 2020. "10-Year Treasury Inflation-Indexed Security, Constant Maturity [DFII10]." Tech. rep., FRED, Federal Reserve Bank of St. Louis. URL https://fred.stlouisfed.org/series/DFII10.

Bright, E. A., P. R. Coleman, A. N. Rose, and M. L. Urban. 2012. "LandScan 2011." Digital dataset: web.ornl.gov/sci/landscan/index.shtml.

Burgess, Robin, Olivier Deschenes, Dave Donaldson, and Michael Greenstone. 2017. "The unequal effects of weather and climate change: Evidence from mortality in India." *NBER Working paper* .

Burke, Marshall, John Dykema, David B Lobell, Edward Miguel, and Shanker Satyanath. 2015. "Incorporating climate uncertainty into estimates of climate change impacts." *Review of Economics and Statistics* 97 (2):461–471.

Carleton, Tamma A and Solomon M Hsiang. 2016. "Social and economic impacts of climate." *Science* 353 (6304):aad9837.

Davis, Lucas W and Paul J Gertler. 2015. "Contribution of air conditioning adoption to future energy use under global warming." *Proceedings of the National Academy of Sciences* 112 (19):5962–5967.

Dell, Melissa, Benjamin F Jones, and Benjamin A Olken. 2014. "What do we learn from the weather? The new climate–economy literature." *Journal of Economic Literature* 52 (3):740–798.

Dellink, Rob, Jean Chateau, Elisa Lanzi, and Bertrand Magné. 2015. "Long-term economic growth projections in the Shared Socioeconomic Pathways." *Global Environmental Change* .

Deryugina, Tatyana and Solomon Hsiang. 2017. "The Marginal Product of Climate." *NBER Working paper* .

Deschenes, Olivier. 2018. "Temperature Variability and Mortality: Evidence from 16 Asian Countries." *Asian Development Review* 35 (2):1–30.

Deschênes, Olivier and Michael Greenstone. 2007. "The economic impacts of climate change: evidence from agricultural output and random fluctuations in weather." *The American Economic Review* 97 (1):354–385.

———. 2011. "Climate change, mortality, and adaptation: Evidence from annual fluctuations in weather in the US." *American Economic Journal: Applied Economics* 3 (October):152–185. URL http://www.nber.org/papers/w13178.

Deschênes, Olivier, Michael Greenstone, and Joseph S Shapiro. 2017. "Defensive investments and the demand for air quality: Evidence from the NOx budget program." *American Economic Review* 107 (10):2958–89.

Deschênes, Olivier and Enrico Moretti. 2009. "Extreme weather events, mortality, and migration." *The Review of Economics and Statistics* 91 (4):659–681.

Diaz, Delavane. 2014. "Evaluating the Key Drivers of the US Government's Social Cost of Carbon: A Model Diagnostic and Inter-Comparison Study of Climate Impacts in DICE, FUND, and PAGE." *Working paper* .

Eurostat. 2013. *Europe in Figures: Eurostat Yearbook 2013*. Publications Office of the European Union.

Fetzer, Thiemo. 2014. "Can workfare programs moderate violence? Evidence from India." .

Gasparrini, Antonio, Yuming Guo, Masahiro Hashizume, Eric Lavigne, Antonella Zanobetti, Joel Schwartz, Aurelio Tobias, Shilu Tong, Joacim Rocklöv, Bertil Forsberg et al. 2015. "Mortality risk attributable to high and low ambient temperature: A multicountry observational study." *The Lancet* 386 (9991):369–375.

Gennaioli, Nicola, Rafael La Porta, Florencio Lopez De Silanes, and Andrei Shleifer. 2014. "Growth in regions." *Journal of Economic Growth* 19 (3):259–309. URL https://ideas.repec.org/a/kap/jecgro/v19y2014i3p259-309.html.

Graff Zivin, Joshua and Matthew Neidell. 2014. "Temperature and the allocation of time: Implications for climate change." *Journal of Labor Economics* 32 (1):1–26.

Guo, Christopher and Christopher Costello. 2013. "The value of adaption: Climate change and timberland management." *Journal of Environmental Economics and Management* 65 (3):452–468.

Guo, Yuming, Antonio Gasparrini, Ben Armstrong, Shanshan Li, Benjawan Tawatsupa, Aurelio Tobias, Eric Lavigne, Micheline de Sousa Zanotti Stagliorio Coelho, Michela Leone, Xiaochuan Pan et al. 2014. "Global variation in the effects of ambient temperature on mortality: a systematic evaluation." *Epidemiology (Cambridge, Mass.)* 25 (6):781.

Heutel, Garth, Nolan H Miller, and David Molitor. 2017. "Adaptation and the Mortality Effects of Temperature Across US Climate Regions." *National Bureau of Economic Research* .

Hsiang, Solomon. 2013. "Visually-weighted regression." *SSRN Working Paper* .

———. 2016. "Climate econometrics." *Annual Review of Resource Economics* 8:43–75.

Hsiang, Solomon, Robert Kopp, Amir Jina, James Rising, Michael Delgado, Shashank Mohan, DJ Rasmussen, Robert Muir-Wood, Paul Wilson, Michael Oppenheimer et al. 2017. "Estimating economic damage from climate change in the United States." *Science* 356 (6345):1362–1369.

Hsiang, Solomon and Robert E Kopp. 2018. "An Economist's Guide to Climate Change Science." *Journal of Economic Perspectives* 32 (4):3–32.

Hsiang, Solomon M and Amir S Jina. 2014. "The causal effect of environmental catastrophe on long-run economic growth: Evidence from 6,700 cyclones." Tech. rep., National Bureau of Economic Research.

Hsiang, Solomon M, Kyle C Meng, and Mark A Cane. 2011. "Civil conflicts are associated with the global climate." *Nature* 476 (7361):438.

Hsiang, Solomon M and Daiju Narita. 2012. "Adaptation to cyclone risk: Evidence from the global cross-section." *Climate Change Economics* 3 (02):1250011.

IIASA Energy Program. 2016. "SSP Database, Version 1.1 [Data set]." Tech. rep., National Bureau of Economic Research. URL https://tntcat.iiasa.ac.at/SspDb.Accessed25December,2016.

Interagency Working Group on Social Cost of Carbon. 2010. "Social Cost of Carbon for Regulatory Impact Analysis - Under Executive Order 12866." Tech. rep., United States Government.

Interagency Working Group on Social Cost of Greenhouse Gases. 2016. "Technical Support Document: Technical Update of the Social Cost of Carbon for Regulatory Impact Analysis." Tech. rep., United States Government.

Isen, Adam, Maya Rossin-Slater, and Reed Walker. 2017. "Relationship between season of birth, temperature exposure, and later life wellbeing." *Proceedings of the National Academy of Sciences* 114 (51):13447–13452.

Jones, Charles I and Peter J Klenow. 2016. "Beyond GDP? Welfare across countries and time." *American Economic Review* 106 (9):2426–57.

Kahn, Matthew E. 2005. "The death toll from natural disasters: the role of income, geography, and institutions." *Review of Economics and Statistics* 87 (2):271–284.

Kopp, Robert E and Bryan K Mignone. 2012. "The US government's social cost of carbon estimates after their first two years: Pathways for improvement." *Working paper* .

Lenssen, N., G. Schmidt, J. Hansen, M. Menne, A. Persin, R. Ruedy, and D. Zyss. 2019. "Improvements in the GISTEMP uncertainty model." *J. Geophys. Res. Atmos.* 124 (12):6307–6326.

Li, Dawei, Jiacan Yuan, and Robert Bob Kopp. 2020. "Escalating global exposure to compound heat-humidity extremes with warming." *Environmental Research Letters* .

Lobell, David B, Michael J Roberts, Wolfram Schlenker, Noah Braun, Bertis B Little, Roderick M Rejesus, and Graeme L Hammer. 2014. "Greater sensitivity to drought accompanies maize yield increase in the US Midwest." *Science* 344 (6183):516–519.

Matsuura, Kenji and Cort Willmott. 2007. "Terrestrial Air Temperature and Precipitation: 1900-2006 Gridded Monthly Time Series, Version 1.01." *University of Delaware*. URL http://climate.geog.udel.edu/climate.

Mendelsohn, Robert, William D Nordhaus, and Daigee Shaw. 1994. "The impact of global warming on agriculture: A Ricardian analysis." *The American Economic Review* :753–771.

Millar, Richard J, Zebedee R Nicholls, Pierre Friedlingstein, and Myles R Allen. 2017. "A modified impulse-response representation of the global near-surface air temperature and atmospheric concentration response to carbon dioxide emissions." *Atmospheric Chemistry and Physics* 17 (11):7213–7228.

Millner, Antony and Geoffrey Heal. 2018. "Time consistency and time invariance in collective intertemporal choice." *Journal of Economic Theory* 176:158–169.

Moore, Frances C and David B Lobell. 2014. "Adaptation potential of European agriculture in response to climate change." *Nature Climate Change* 4 (7):610.

Murphy, Kevin M and Robert H Topel. 2006. "The value of health and longevity." *Journal of Political Economy* 114 (5):871–904.

National Academies of Sciences, Engineering, and Medicine. 2017. *Valuing Climate Damages: Updating Estimation of the Social Cost of Carbon Dioxide*. Washington, DC: The National Academies Press. URL https://www.nap.edu/catalog/24651/valuing-climate-damages-updating-estimation-of-the-social-cost-of.

Newell, Richard G and William A Pizer. 2004. "Uncertain discount rates in climate policy analysis." *Energy Policy* 32 (4):519–529.

Nordhaus, William D. 1992. "An optimal transition path for controlling greenhouse gases." *Science* 258 (5086):1315–1319.

Park, R Jisung, Joshua Goodman, Michael Hurwitz, and Jonathan Smith. 2020. "Heat and learning." *American Economic Journal: Economic Policy* 12 (2):306–39.

Pindyck, Robert S. 2013. "Climate change policy: What do the models tell us?" *Journal of Economic Literature* 51 (3):860–872.

Rasmussen, D. J., Malte Meinshausen, and Robert E. Kopp. 2016. "Probability-weighted ensembles of U.S. county-level climate projections for climate risk analysis." *Journal of Applied Meteorology and Climatology* 55 (10):2301–2322. URL http://journals.ametsoc.org/doi/abs/10.1175/JAMC-D-15-0302.1.

Riahi, Keywan, Detlef P Van Vuuren, Elmar Kriegler, Jae Edmonds, Brian C O'neill, Shinichiro Fujimori, Nico Bauer, Katherine Calvin, Rob Dellink, Oliver Fricko et al. 2017. "The shared socioeconomic pathways and their energy, land use, and greenhouse gas emissions implications: an overview." *Global Environmental Change* 42:153–168.

Rohde, Robert, Richard Muller, Robert Jacobsen, Saul Perlmutter, Arthur Rosenfeld, Jonathan Wurtele, J Curry, Charlotte Wickham, and S Mosher. 2013. "Berkeley Earth temperature averaging process." *Geoinfor Geostat: An Overview* 1 (2):1–13.

Schlenker, Wolfram and Michael J Roberts. 2009. "Nonlinear temperature effects indicate severe damages to US crop yields under climate change." *Proceedings of the National Academy of Sciences* 106 (37):15594–15598.

Schlenker, Wolfram, Michael J Roberts, and David B Lobell. 2013. "US maize adaptability." *Nature Climate Change* 3 (8):690–691.

Sheffield, Justin, Gopi Goteti, and Eric F Wood. 2006. "Development of a 50-year high-resolution global dataset of meteorological forcings for land surface modeling." *Journal of Climate* 19 (13):3088–3111.

Sherwood, Steven and Qiang Fu. 2014. "A drier future?" *Science* 343 (6172):737–739.

Sherwood, Steven C and Matthew Huber. 2010. "An adaptability limit to climate change due to heat stress." *Proceedings of the National Academy of Sciences* 107 (21):9552–9555.

Solon, Gary, Steven J Haider, and Jeffrey M Wooldridge. 2015. "What are we weighting for?" *Journal of Human Resources* 50 (2):301–316.

Stern, Nicholas. 2006. *The Economics of Climate Change: The Stern Review*. Cambridge University Press.

Taylor, Karl E, Ronald J Stouffer, and Gerald A Meehl. 2012. "An overview of CMIP5 and the experiment design." *Bulletin of the American Meteorological Society* 93 (4):485.

Tebaldi, Claudia and Reto Knutti. 2007. "The use of the multi-model ensemble in probabilistic climate projections." *Philosophical Transactions of the Royal Society of London A: Mathematical, Physical and Engineering Sciences* 365 (1857):2053–2075. URL http://rsta.royalsocietypublishing.org/content/365/1857/2053.

Thomson, Allison M., Katherine V. Calvin, Steven J. Smith, G. Page Kyle, April Volke, Pralit Patel, Sabrina Delgado-Arias, Ben Bond-Lamberty, Marshall A. Wise, Leon E. Clarke, and James A. Edmonds. 2011. "RCP4.5: a pathway for stabilization of radiative forcing by 2100." *Climatic Change* 109 (1):77. URL https://doi.org/10.1007/s10584-011-0151-4.

Thrasher, Bridget, Edwin P Maurer, C McKellar, and PB Duffy. 2012. "Technical note: Bias correcting climate model simulated daily temperature extremes with quantile mapping." *Hydrology and Earth System Sciences* 16 (9):3309–3314.

Tol, Richard S.J. 1997. "On the optimal control of carbon dioxide emissions: an application of FUND." *Environmental Modeling & Assessment* 2 (3):151–163. URL http://dx.doi.org/10.1023/A:1019017529030.

Traeger, Christian P. 2014. "Why uncertainty matters: discounting under intertemporal risk aversion and ambiguity." *Economic Theory* 56 (3):627–664.

United Nations. 2017. "World Mortality 2017." Tech. rep., United Nations Economic and Social Affairs.

U.S. Environmental Protection Agency. 2016a. "Recommended Income Elasticity and Income Growth Estimates: Technical Memorandum." Tech. rep., U.S. Environmental Protection Agency Office of Air and Radiation and Office of Policy.

———. 2016b. "Valuing mortality risk reductions for policy: A meta-analytic approach." Tech. rep., U.S. Environmental Protection Agency Office of Policy, National Center for Environmental Economics.

Van Vuuren, Detlef P, Jae Edmonds, Mikiko Kainuma, Keywan Riahi, Allison Thomson, Kathy Hibbard, George C Hurtt, Tom Kram, Volker Krey, Jean-Francois Lamarque et al. 2011. "The representative concentration pathways: An overview." *Climatic Change* 109 (1-2):5.

Viscusi, W Kip. 2015. "The role of publication selection bias in estimates of the value of a statistical life." *American Journal of Health Economics* .

Weitzman, Martin L. 2011. "Fat-tailed uncertainty in the economics of catastrophic climate change." *Review of Environmental Economics and Policy* 5 (2):275–292.

WHO. 2018. "Global Health Estimates 2016: Deaths by cause, age, sex, by country and by region, 2000–2016." Tech. rep., World Health Organization.

Yuan, Jiacan, Michael L Stein, and Robert E Kopp. 2019. "The evolving distribution of relative humidity conditional upon daily maximum temperature in a warming climate." .